AD-A150 530 TESTS OF TURBULATORS FOR FIRE-TUBE BOILERS(U) IOWA STATE UNIV AMES HEAT TRANSFER LAB G H JUNKHAN ET AL. OCT 82 HTL-29 1/1

UNCLASSIFIED F/G 13/11 NL

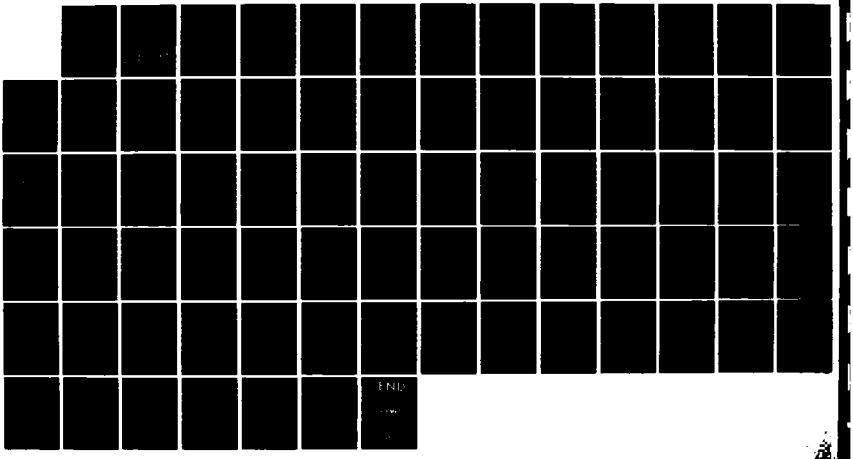

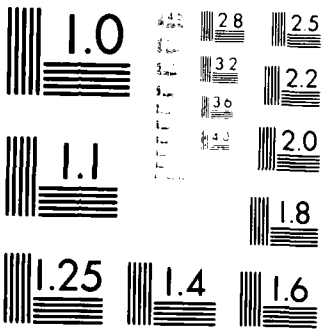

October 1982

G. H. Junkhan
A. E. Bergles
V. Nirmalan
T. Ravigururajan

Tests of Turbulators for Fire-Tube Boilers

HTL-29
ISU-ERI-Ames-83130

U.S. Army
Contract No. DAAK 70-81-C-0219
FESA-E-83023

final report

College of Engineering
Iowa State University

Final Report

G. H. Junkhan
A. E. Bergles
V. Nirmalan
T. Ravigururajan

Tests of Turbulators for Fire-Tube Boilers

October 1982

HTL-29
ISU-ERI-Ames-83130

U.S. Army
Contract No. DAAK 70-81-C-0219
FESA-E-83023

Heat Transfer Laboratory
Department of Mechanical Engineering
Engineering Research Institute
Iowa State University, Ames

SUMMARY

One of the most attractive modifications for fire tube boilers is the introduction of "turbulators" into the boiler tubes. These inserts increase gas-side heat transfer coefficients, thereby increasing the heat removed from the flue gases. Assuming that the equipment is properly operated and adjusted, the boiler efficiency will be higher. Although several types of twisted metal strips are quite widely used as original equipment or as retrofit hardware, heat transfer coefficients and friction factors are not available in the open literature. This information was obtained in the present study for three popular turbulator inserts.

An electrically heated flow facility was developed to deliver hot air to a water-cooled steel tube of 2.675 in. i.d. and 71.75 in. length. Tube wall temperatures, fluid bulk temperatures, and flow rates were measured. The cooling coil was segmented so that sectional average heat transfer coefficients could then be derived for four regions of the tube.

Reference data for the empty tube are in excellent agreement with the usual correlations. Two commercial turbulators, consisting of narrow, thin metal strips bent and twisted in zig-zag fashion to allow periodic contact with the tube wall, displayed 125 and 157% increases in heat transfer coefficients at a Reynolds number of 10,700. Insert orientation had at most a 10% effect on the heat transfer coefficient. A third commercial turbulator, consisting of a twisted strip with width slightly less than tube diameter, provided a 60% increase in heat transfer coefficient. The friction factor increases accompanying these heat

transfer coefficient increases were 1110%, 1000%, and 120%, respectively. These data should be helpful in assessing the overall performance gains to be expected when the turbulators are used in actual boilers.

HTL-29

LIST OF ILLUSTRATIONS

A-1

LIST OF TABLES

INTRODUCTION

Background

The U.S. Army is activ ly pursuing hardware and strategies which will lead to the reduction of fuel oil used for space heating. Eventually, many of the oil-fired plants will be replaced with systems fired by coal. In the interim, however, it is important to minimize oil consumption.

One of the most attractive boiler modifications is the introduction of "turbulators" into the boiler tubes. One popular configuration is a narrow, thin metal strip bent and twisted in zig-zag fashion to allow periodic contact with the tube wall. Twisted ribbons or tapes, of tube diameter width, have been used for a century. Another simple insert is a coiled wire similar to a spring. These inserts increase the gas-side heat transfer coefficients, thereby increasing the heat recovery from the flue gases. Assuming that the equipment is properly operated and adjusted, there will be a higher boiler efficiency. Of course, boiler performance will reflect the increased flow friction of the turbulators.

Turbulator inserts are advertised in rather glowing terms, with typical claims of up to 15% savings in fuel based on field operational data. Unfortunately, the accuracy of such field tests is open to question. Furthermore, it does not appear that heat transfer and fluid flow characteristics of the major turbulator inserts have been reported in the open literature. For these reasons and the fact that boilers for military installations operate at low heat fluxes, the Army, through the U.S. Army Facilities Engineering Support Agency (FESA) has

embarked on an evaluation program to determine the actual energy savings to be expected from the installation of turbulators.

It is the intent of this evaluation program to estimate what the fuel reduction "could be" for any boiler on a seasonal basis, rather than what the reduction is during a short period of steady-state operation. Rather than test an actual boiler, the Army program will use National Bureau of Standards computer models to simulate boiler performance. As preliminary input, typical published values of the gas-side heat transfer coefficient and friction factor for twisted tapes and wire coils were utilized. Actual values of the thermal-hydraulic performance of commercial turbulators were then measured in the Iowa State University Heat Transfer Laboratory. The measurements were carried out for a smooth tube and for the same tube with various inserts under conditions of cooling of a hot gas at flow rates representative of actual boilers. This report concerns the findings of the Iowa State Heat Transfer Laboratory experiments for three commercially available inserts.

Turbulators to be Tested

Three turbulator inserts were provided to the Heat Transfer Laboratory by FESA. These inserts are offered commercially; however, detailed thermal-hydraulic performance data do not appear to be available in the open literature. The manufacturers or distributors of the inserts and their addresses are given in Appendix A.

The somewhat complex geometric characteristics of the inserts are given in Figs. 1 through 3, where the nomenclature used is noted on each figure and a letter symbol is used to identify each insert. Numerical values of the various geometric dimensions are given in Table I. Insert pitch is defined in various ways in the references cited in this report. In order to have a uniform basis for comparison, this report uses diametral pitch: the number of inside tube diameters along the tube axis in which one full twist (360°) of a twisted tape or one full cycle of a bent strip turbulator occurs.

Table I. Insert characteristics.

Property		Insert		
		Type A Fig. 1	Type B Fig. 2	Type C Fig. 3
Length	in.	72.5	73.0	74.5
Tube span	in.	2.62	2.56	2.60
Pitch (for 2.675 in. i.d. tube)		4.02	2.80	10.47
Width	in.	0.880	0.755	2.60
Thickness	in.	0.075	0.085	0.055
Longitudinal Angle	deg	122°	100°	-
Primary Twist Angle	deg	±25°	30°	-
Secondary Twist Angle	deg	-	-30°	-

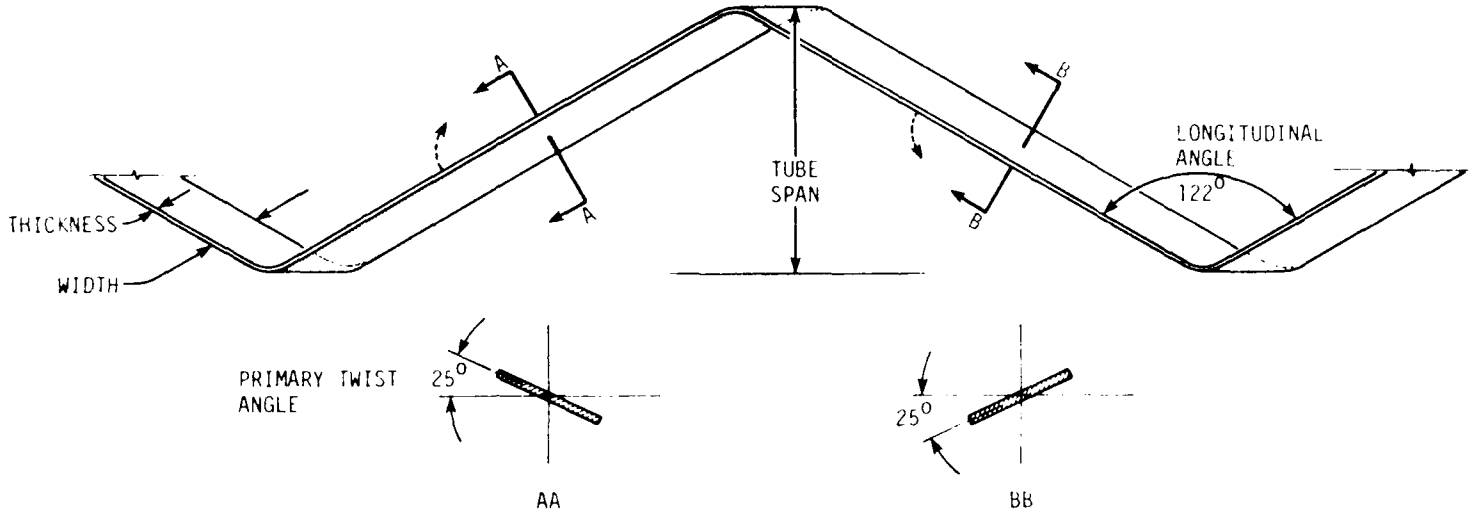

Fig. 1. Geometry of Type A insert (not to scale).

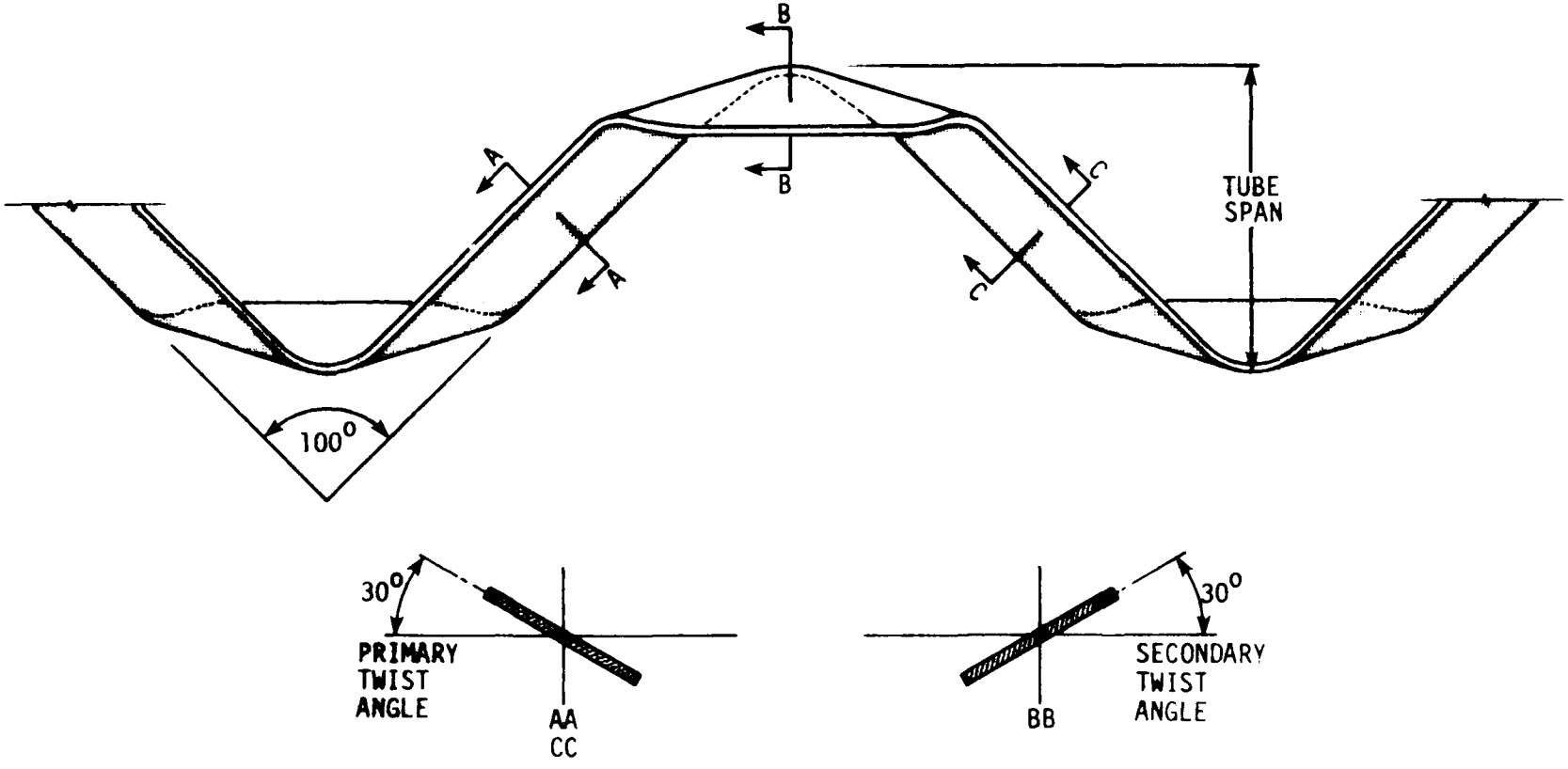

Fig. 2. Geometry of Type B insert (not to scale).

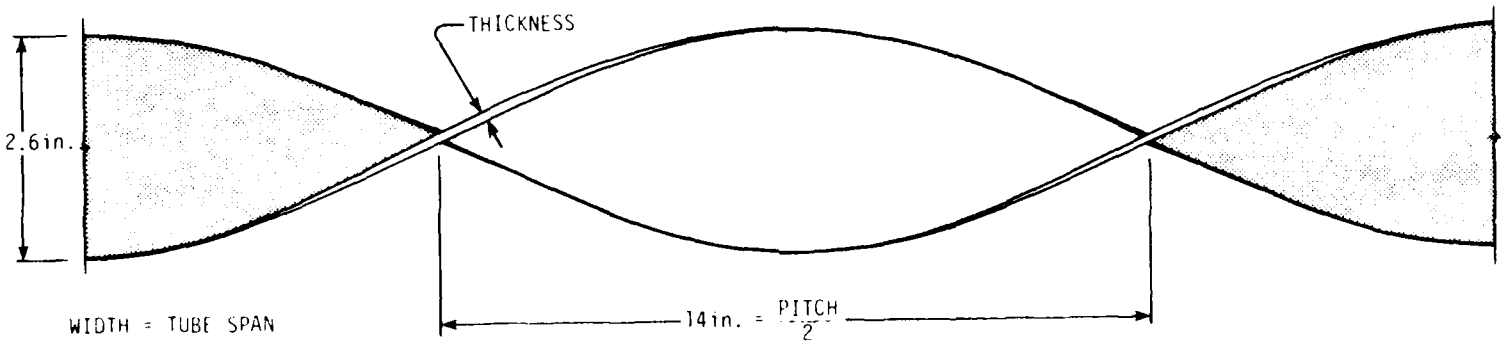

Fig. 3. Geometry of Type C insert (not to scale).

LITERATURE REVIEW

A literature search on the effects of tube inserts of various types suitable for augmentation of gas heat transfer coefficients in fire tube boilers was conducted using the current Computerized Bibliography on Augmentation of Convective Heat and Mass Transfer [1]. Inserts most applicable to the present investigation of fire tube boiler turbulators are forms of twisted tapes and wire coils. Some early studies report complete boiler tests with and without twisted-tape turbulators. The incentive was to confirm on a stationary boiler the advantages of the marine practice of using "retarders."

Whitham [2] in 1896 inserted "loosely fitting" and gently twisted (1 turn in 10 ft) tapes in the 44-4 in. horizontal tubes of a 100 hp boiler. The saving of fuel with turbulators was as much as 8%, with the improvements being observed only when "the boiler plant is pushed and the draught is strong." These general conclusions were reinforced over 50 years later by Kirov [3] who fitted an Economic Boiler having 76-2.74 in. i.d. tubes with 2.5 in. width twisted tapes of 1 turn in 1.17 ft or 1 turn in 2.33 ft. With full-length tapes, the increase in boiler efficiency[1] was 5 to 7 percentage points[2], which was equivalent to a fuel saving of 7 to 10%. The increase in fan horsepower was negligible for the forced draft system under test; however, use of the retarders in a natural draft system was not advised.

---

[1] Boiler efficiency is defined as the heat transferred to the water divided by the heat available from the fuel consumed.

[2] Based on higher heat of combustion of the coal, as fired.

In a recent study conducted for DOE at Brookhaven National Laboratory, it was found that the addition of turbulators to residential oil-fired boilers resulted in fuel savings of 2-8% [4]. Details are not given in the report.

Actual heat transfer and flow friction data found for twisted tapes and wire coils in air flows are described below; these are the only cases found with air as the working fluid and with cooling. Other data using water as the working fluid have been obtained, but they are not considered useful to this investigation.

Wire Coils

Early work on this type of enhancement was performed by Colburn and King [5] on conically shaped copper wire coils. Wire was wound in a three-dimensional conical helix, beginning with a coil of essentially the same circumference as the inside of the 2.625 in. i.d.test section and progressing to the apex of the cone in ever-decreasing radii. The altitude of the cone thus formed was about 4 in. Nine of these coils were placed in the 3 ft long test section in an apex-to-base sequence. No information is given on wire diameter, nor on the direction of flow relative to the cone sequence in the test section.

The test fluid was air, heated by electrical resistance heaters. The test section was water-cooled by a helically-wound copper tube soldered to the outside, with end losses and axial conduction losses reduced by using guard coolers on sections of tube just upstream and downstream of the test section. Tube wall temperatures were measured

on the outside wall of the tube at five equally-spaced axial locations by the thermocouples embedded in the solder between copper cooling coils. Entering air temperature was measured by obtaining an average of temperatures read from a thermocouple traversed along a diameter of the tube. The exit gas temperature was taken from thermocouple readings in an insulated mixing chamber at the test section outlet. Inlet air temperatures ranged from 107 to 390°C, and inlet wall temperatures varied from 9.2 to 11.5°C.

Data are reported as curves of $\bar{h}_a/c_p$ and pressure drop corrected for kinetic energy losses as functions of mass velocity through the test section. The data are also given in tabular form. Recast in the more familiar form of $Nu_D/(Pr)^{0.4}$ and f as functions of Re_D based on average fluid properties, the data are shown in Figs. 4 and 5.

Twisted Tapes

An early, but comprehensive study of twisted-tape inserts was reported by Royds [6]. Electrically heated air was allowed to flow through a tube of 2.31 in. i.d. and 6.58 ft length. The last section was cooled by water flowing in a shell around the tube. The inlet air temperature was measured by a calibrated platinum resistance thermometer. Other temperatures were obtained by calibrated mercury-in-glass thermometers. A large number of tests were made with inlet air temperatures varying from 430°F to 1000°F.

Nine different sooted twisted tapes of 1.94-in. width were tested with pitches varying from 4.72 to 38.5. The results obtained show

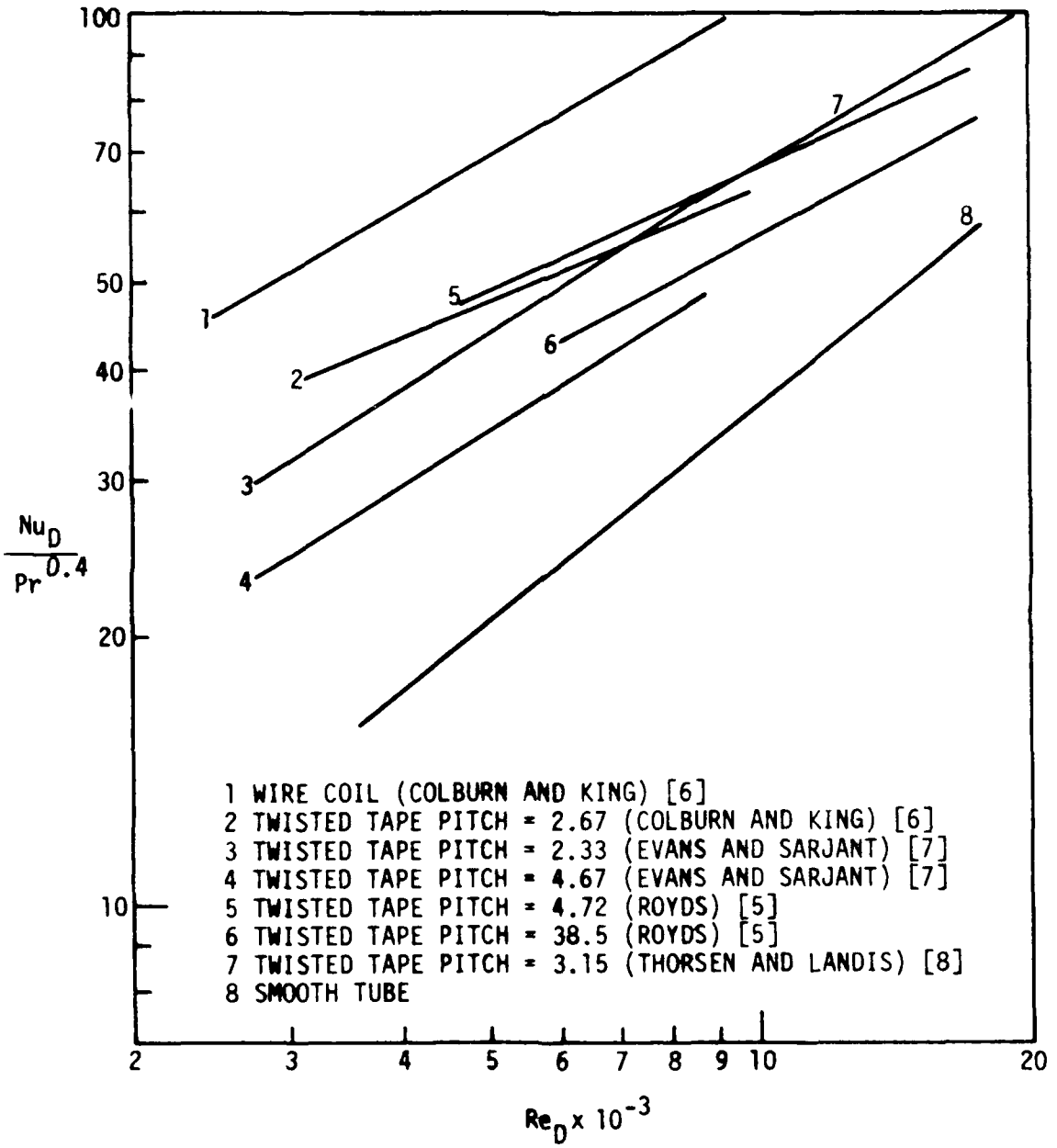

Fig. 4. Comparison of published heat transfer data for wire coils and twisted tapes.

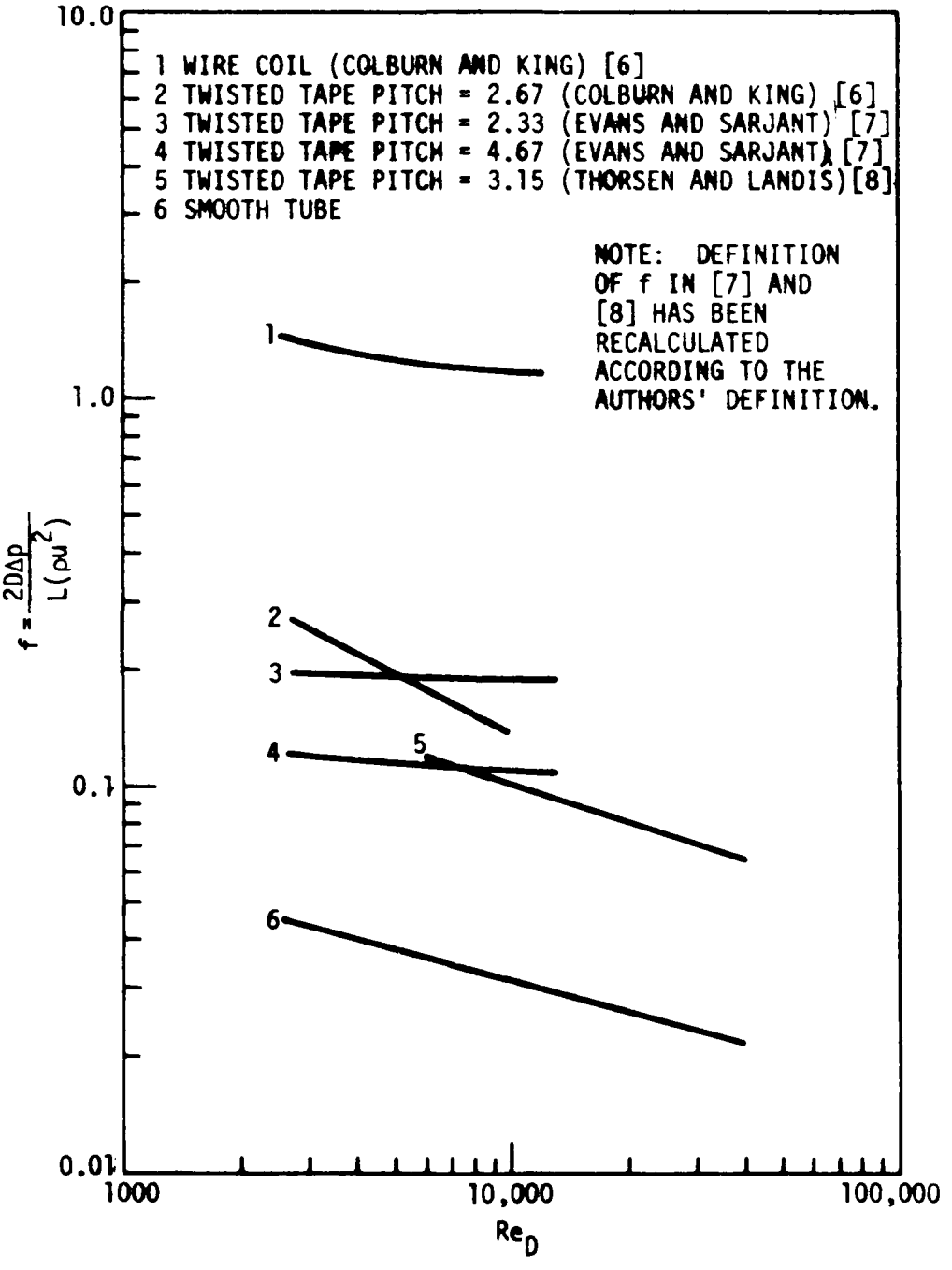

Fig. 5. Comparison of published friction factor data for wire coils and twisted tapes. (Data converted to same base for f.)

that pitches larger than about 8.66 had very little influence on the heat transfer. Data were reported as curves of heat transfer coefficient as a function of mass velocity. The pressure drop data are also given as a function of mass velocity. These pressure drop data were not corrected for kinetic energy losses. To compare Royd's results in the form of $Nu_D/Pr^{0.4}$ as a function of Re_D, the bulk temperature was assumed to be 550°F. These data are given in Fig. 4. The pressure drop data are not included in Fig. 5 as it was not possible to determine the necessary corrections for kinetic energy losses.

Colburn and King [5] also investigated enhancement effects of twisted tapes using the same apparatus outlined in the preceding section. Two full length, apparently snug fitting tapes were tested; however, data were tabulated for only one of these tapes. Data were taken for inlet air temperatures ranging from 108°C to 392°C and inlet tube wall temperatures from 9.3°C to 12.3°C. As with wire coil enhancement, data are presented both graphically and tabularly as $\bar{h}_a/c_p$ and corrected pressure drop as functions of mass velocity through the test section. Data, recalculated as $Nu_D/((Pr)^{0.4}$ and f as functions of Re_D are included in Figs. 4 and 5 for a 3 ft long steel tape with a pitch of 2.67 in the 2.625 in. i.d. tube.

Studies on twisted tape enhancement were also conducted by Evans and Sarjant [7] using electrically-heated air in an apparatus somewhat similar to that of Colburn and King. Tapes of 2.5 in. width, with pitches of 2.33, 3.00, 4.00, and 4.67, were tested in an 8 ft long, 3 in. i.d. test section. The outside of the tube was water cooled by helically-wound copper tubing soldered on the surface. Provision was

made for making radial gas temperature and velocity measurements at several (unspecified) axial locations so that bulk temperature and mean velocity could be calculated. Energy balances between cooling water energy gain and air energy loss were used to validate data for each run. Inlet air temperatures were approximately 700°F, while inlet Reynolds numbers varied from about 3000 to 13,000.

Results are presented as curves of convective heat transfer coefficient and pressure drop corrected for kinetic energy losses as functions of Reynolds number for different twisted tapes. Data for twisted tape pitches of 2.33 and 4.67 were converted to $Nu_D/(Pr)^{0.4}$ as a function of Re_D and are shown in Fig. 4. Friction factor data for the same tapes are shown in Fig. 5.

Evans and Sarjant attempted to separate the effects of radiation and convection in twisted tape enhancement. While noting that their analysis is not conclusive in this respect, they estimated the maximum contribution of radiation as 25 percent of the measured heat transfer coefficient when gas temperatures above about 1000°F were encountered. The contribution of radiation drops rapidly as gas temperature is reduced.

More recent tests of the effects of twisted tapes on cooled air flows were reported by Thorsen and Landis [8]. Air was supplied at temperatures up to 475°F to a 1 in. i.d. water cooled tube. Twisted tape pitches were 3.15, 5.17, and 8.00, and the tube-tape gap was about 0.003 in. Heat transfer and friction factor data for the smallest pitch tape are given in Figs. 4 and 5, respectively. The following empirical correlations were given to describe the data.

$$Nu_D = 0.023[fn_1(D,H)]Re_D^{0.8}\ Pr^{1/3}\left(\frac{\bar{T}_s}{\bar{T}_b}\right)^{-0.1}(1 - 0.25\ \frac{\sqrt{Gr}}{Re_D}) \qquad (1)$$

$$f = \frac{0.046}{Re_D^{0.2}}\left(\frac{\bar{T}_s}{\bar{T}_b}\right)^{-0.1}[fn_2(D,H)] \qquad (2)$$

where $fn_1(D,H)$ and $fn_2(D,H)$ are given in [8]. A major concern of this work was assessment of the effects of variable properties. The temperature ratio correction factor was determined primarily from heating data due to the limited values of (T_s/T_b) which could be attained in cooling. The maximum value of $(T_s/T_b)^{-0.1}$ for cooling was 1.05; however, the scatter of the data was at least 5%.

Mechanism of Enhancement

Wire coils are a popular turbulator insert. In the usual case where the coils are uniform in diameter and in contact with the tube wall, the wire acts as a roughness element. The flow separation and reattachment are similar to that produced by integral roughness elements created by rolling or swaging. The wires are usually in poor thermal contact with the tube; however, the fin effect of any of these roughness elements is rather small. At usual velocities, the flow is predominantly axial rather than a swirl flow which follows the coil. A heat transfer - momentum transfer analogy solution is available for helical repeated ribs [9], but it has not been tested against coil data. Although analytical results are available for the effect of

variable properties in cooled gas flows [10], there are no data for cooling in tubes which have repeated rib roughness.

Wire coils with varying radii function more as displaced enhancement devices, as all but one coil in each element disturb the core flow rather than the boundary layer at the wall. The eddies produced in the core are expected to have some influence on transport of momentum and energy at the wall; however, the effect is probably less than if all coils were at the wall. No models have been proposed for this situation.

Twisted tapes enhance heat transfer by creating a higher velocity due to the longer path length, by introducing a secondary flow due to the centrifugal force acting on a variable density fluid, and by utilizing the fin effect of the tape. In the tests reported above, the centrifugal force actually reduces the heat transfer from the air flow. Fin effects are generally small because the tape-tube gaps are usually rather large so that the tapes can be easily inserted and removed. No analyses have considered all of these factors; hence, empirical correlations are utilized, e.g. [8], which also includes a correction for temperature-dependent properties.

APPARATUS

An apparatus has been developed to determine the thermal-hydraulic performance of various turbulator inserts with cooling of air. The test rig consists basically of a blower suitable to produce Reynolds

numbers of order 10,000, a heater box to heat the air to over 300°F, and the actual test section where the performance of the inserts is to be evaluated. The cooling water jacket of the test section simulates fire-tube boiler conditions while serving as a calorimeter.

Flow System

The U-shaped flow system to provide hot air to the test section is depicted in Fig. 6. Airflow is provided by a centrifugal blower that delivers 600 SCFM at a head of 6 in. of water. After leaving the fan, the air passes through flow straighteners and a flow development length of 10 ft before entering an orifice meter. Eight feet downstream from the orifice meter, the air passes through an elbow before entering the heater box.

The heater box was fabricated from 22 gage sheet steel in three parts: an inlet rectangular diffuser section varying in cross section from 6 in. × 6 in. at the entrance to 21 in. × 11 1/4 in. over a length of 72 in. The flow is at low velocity as it enters the 8 in. long section containing a Chromalox Process Air Duct Heater, Model ADHT-010XX, rated at 10 KW, 240 V, 3 phase. The box cross section is reduced from 21 in. × 11 1/4 in. back to 6 in. × 6 in. over a length of 50 in. downstream of the heater. Each part of the box was fabricated in two halves and joined by welding along the center.

Three autotransformers are connected in a 208 V Delta circuit to provide the electrical input to the heater. High temperature insulating gasket material is used to prevent direct contact between the heater and

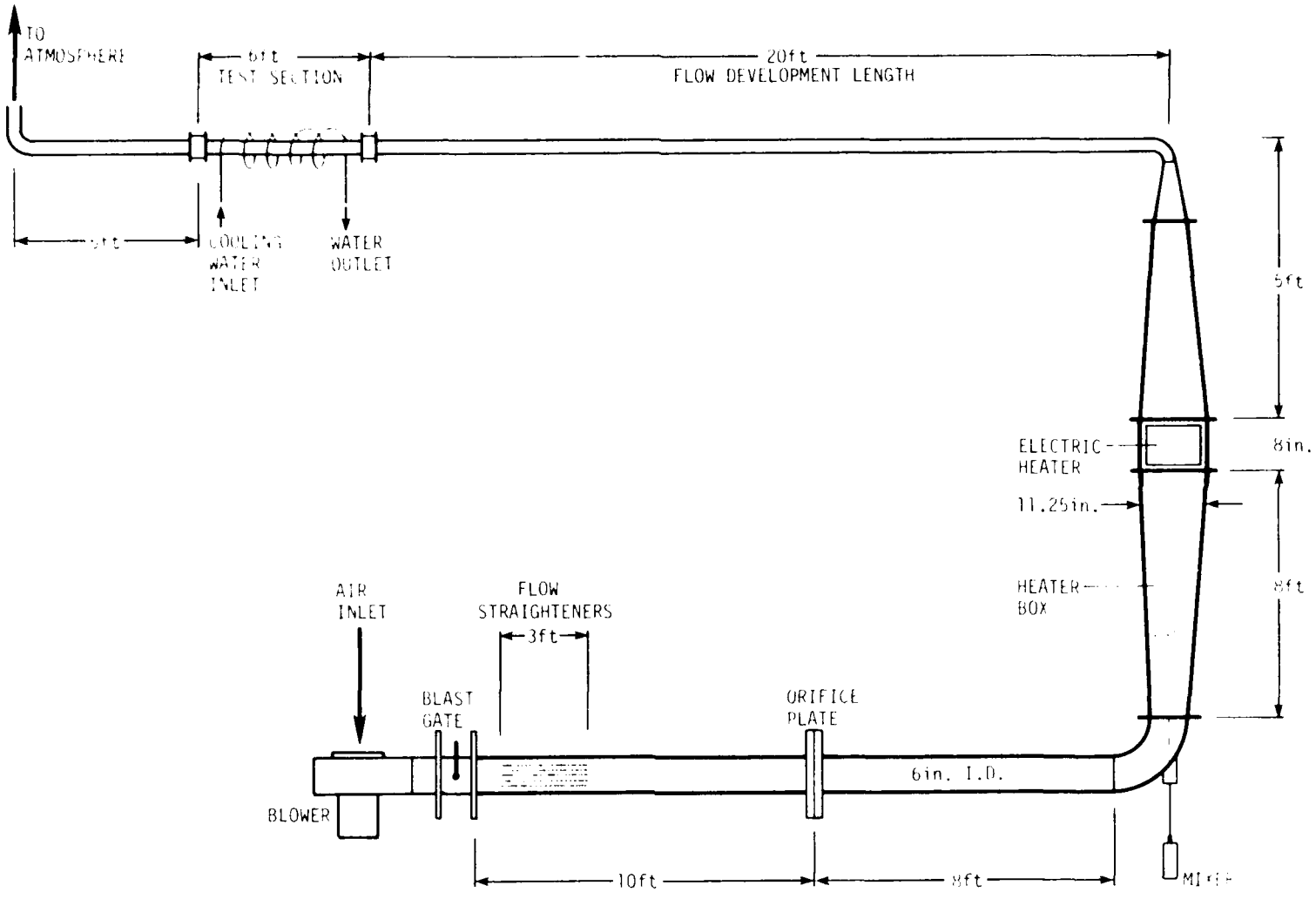

Fig. 6. Flow system (not to scale).

the duct. An over-temperature protector is included in the electrical circuit to cut off electrical power to the heater once a predetermined temperature is reached. A motorized mixer is provided to minimize thermal stratification within the heater duct.

The hot air coming out of the heater box passes through a bend into a developing length of 20 ft before entering the test section. After passing through the test section, the air is exhausted into a 5 ft long pipe section before discharge outside the building. The heater box and piping leading into and out of the test section are insulated with calcium silicate blocks capable of withstanding temperatures of more than 1500°F. These blocks are covered with an additional layer of glass fiber to reduce the heat loss to a minimum.

The test section is insulated simply with glass fiber since the outside temperature of the calorimeter is less than 150°F. Precautions were also taken to insulate the hypodermic tubing carrying thermocouple leads for measuring temperatures.

Test Section

The test section shown in Fig. 7 is based on a 3 in. o.d. carbon, drawn-on-mandrel steel tube with i.d. of 2.675 in. to provide a snug fit with the inserts provided. The tube is 71 3/4 in. long and is flanged at the ends to facilitate installation and removal of inserts. Each end of the tube is fitted with three pressure taps spaced equally around the circumference. Tube wall temperatures are measured with chromel/alumel thermocouples fitted into axial slots milled part way

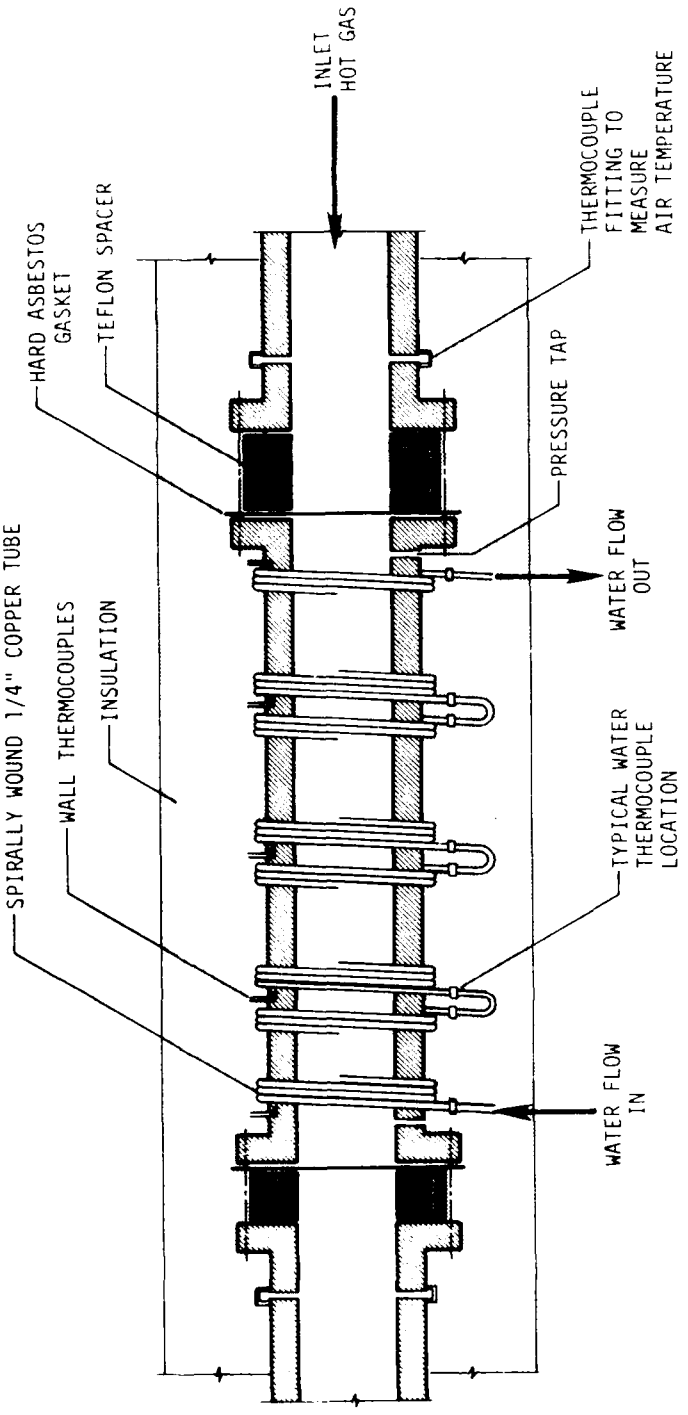

Fig. 7. Test section schematic (not to scale).

through the tube wall. Five axial locations for these thermocouples were chosen to correspond with the water calorimeter cooling sections described below. Three thermocouples were installed at each axial location, spaced equally around the tube circumference. The thermocouples were made of welded junctions and were inserted into the slots through small tubes passing under the calorimeter cooling sections.

The water calorimeter for cooling the gas and conducting energy balances is made of 1/4 in. i.d. copper tubing wound around the tube. Prior to installation, the outside of the steel tube was cleaned and tinned. Then the copper tube was soldered to the outside with a low temperature (430°F) silver bearing solder, All State No. 430 with Duzall liquid flux. Heating was by a torch; to facilitate rotation, the tube was installed in a lathe and the copper tubing was soldered to the steel tube as it was being tightly wound.

The calorimeter tubing was connected as four separate subsections in series, with water temperature measured at the inlet and outlet of each subsection. This feature, together with the wall thermocouples installed as described above, permitted the determination of four sectional-average gas side heat transfer coefficients.

Instrumentation

The basic measurements needed are the air and water mass flow rates and the various air and water bulk temperatures. Also required for calculation of the heat transfer coefficients are the wall temperatures.

Additionally, the pressure drop is required to calculate the friction factor.

The air flow is controlled by a blast gate at the blower outlet and passes through flow straighteners before entering the section upstream of the ASME orifice. The pressure drop across the orifice is monitored by a differential pressure transducer, which is connected via a Scanivalve to a piezometer ring attached to the multiple pressure taps. The same system was used to measure static pressure. The mass flow rate was found using standard ASME procedures and equations. Also measured were the static pressure at the test section inlet and pressure drop across the test section.

The temperatures measured are the wall temperatures along the test section, inlet and outlet air temperatures, water temperatures at the inlet and outlet of each segment of calorimeter tubing, and the room temperature. Thermocouples are made of 28 ga chromel/alumel wire, referenced to a 150°F Whitaker reference junction. Both temperature and pressure signals were recorded digitally by the Heat Transfer Laboratory Data Acquisition System [11]. Finally, the water flow rate was measured directly using a container on a sensitive balance and a stopwatch.

Some of the problems anticipated in the apparatus were air leaks, stratification of air flow in the heater box, axial conduction of heat to the test section, and radiation errors in temperature measurements. The absence of air leaks was confirmed by comparing air flow measured by the orifice downstream of the blower with flow measured at the exhaust

(past the test section) using a pitot tube and taking a velocity profile. The difference was less than one percent.

As noted earlier, a mixer was introduced into the heater to heat the air more uniformly. This avoided early tripping of the power supply by the over-temperature protector, whose sensing thermocouple is located in the middle of a heater element at the downstream last row of vertically heated elements. To minimize the axial conduction from the test section, two teflon spacers, 2 1/2 in. and 1 1/2 in. thick, were placed at the inlet and outlet of the test section, respectively. Four thermocouples were inserted on either side to measure the temperature drop across the spacers so that the axial conduction could be estimated. Regarding the influence of radiation on temperature measurements, calculations showed that the errors were very small and well within the experimental error margin.

Procedure

Testing and Data Acquisition

After starting the blower and the water pump, the electrical heater was switched on. The over-temperature controller was set previously. Initially, the air flow was kept low so that the system could warm up faster. Normally, the time taken for the air temperature at the test section inlet to reach 300°F was approximately three hours. The stirrer raised the temperature of the air considerably (sometimes up to 40°F) through uniform mixing around the heater. The flow rate was then adjusted for the run requirements. When steady state was reached,

the temperature drop from the heater box to the test section was less than 25°F. Whenever the flow rate (Reynolds number) was subsequently changed, it took about twenty minutes to attain steady-state conditions on both air and water sides. The water flow rate was set at about 0.2 gpm which represented a good compromise between an accurately measurable temperature rise and a nearly isothermal tube wall.

Once the steady state was reached, the reading of various temperatures and pressures could be done in about one minute through the data acquisition system. The system used was identical to the one described in Reference 11, with the exception of the digital voltmeter, which was a more recent model. A program was written which enabled the system to take all the required measurements as well as reduce them to relevant information. The program flow chart and listing are given in Appendix B.

Data Reduction

The computer was instructed to scan inlet air and outlet water temperatures for steady state. At steady state, all thermocouples and previous transducer readings were read, quantities were calculated, and the heat balance was checked:

$$q_w - q_c = q_a \tag{3}$$

Agreement to within 5% was required to validate a run. (Most energy balances agreed to within 2-3%.) If acceptable, the data reduction was concluded and the results were printed out.

Average heat transfer coefficients were determined for each calorimeter segment of the test section. Starting at the first segment, the energy added to the water is obtained from $q_w - q_c = \dot{m}_w c_{pw}(T_{w2} - T_{w1})$

where q_c is the estimated heat transfer to the water by conduction from the upstream ducting, $q_c = k_t A(\Delta T_t/\Delta X)$. Assuming that $q_w = q_a = \dot{m}c_{pa}(T_{a1} - T_{a2})$, T_{a2} can be calculated. This involves iteration since the air specific heat is dependent on temperature. The average surface temperature, $\bar{T}_s$, is taken as the average of the two average temperatures for the two measuring stations in each section, that is, the linear average of 6 readings. The heat transfer coefficient, $\bar{h}_a$, is then obtained from the usual expression

$$q_a = \left[\frac{1}{\bar{h}_a \pi D\, L_c} + \frac{1}{2\pi k_s L_c}\, \ell n\left(\frac{D_t}{D}\right)\right]^{-1} \left[\frac{(\bar{T}_s - T_{a1}) - (\bar{T}_s - T_{a2})}{\left(\ell n \frac{\bar{T}_s - T_{a1}}{\bar{T}_s - T_{a2}}\right)}\right] \tag{4}$$

The process is repeated using the outlet air temperature at one section as the inlet temperature for the next section. The second and third segments have no conduction correction; however, there is heat gain by the coolant in the fourth section.

In calculating the Reynolds number, no allowance was made for the blockage of turbulators. The average Fanning friction factor is given by

$$f = \frac{\Delta p D \rho\, A_x^2}{2\, L\, \dot{m}_a^2} \tag{5}$$

where the measured pressure drop is corrected for the momentum change. Again, the cross-sectional area is that of the empty tube without consideration of turbulators.

Uncertainties in Nusselt number, Prandtl number, Reynolds number and friction factor were estimated from a typical run at Re = 12,500. The uncertainties given below are typical of the uncertainties that can be expected in other test runs.

Term	Uncertainties
Nu	±5%
Re	±3%
Pr	±3.5%
f	±5.3%

Error analysis details and sample calculations are given in Appendix D.

RESULTS AND DISCUSSION

Results

Before starting to evaluate the performance of the inserts, the experimental apparatus was tested for its performance as a plain tube without using inserts. Flows for Reynolds numbers from 6,000 to 25,000 were tested. Heat transfer and friction characteristics were determined for nominal inlet air temperatures of 330°F. Errors in the energy balance were under five percent, with most balances falling within two or three percent. The results compared favorably with the well-accepted equation of Dittus and Boelter [12],

$$Nu_D = 0.023(Re_D)^{0.8}(Pr)^{0.3} \qquad (6)$$

as shown in Fig. 8. Experimental data for Fig. 8 are given in tabular form in Appendix C.

Test runs were conducted over a range of Reynolds numbers for the three inserts. The reduced data were plotted as curves of Nu_D vs. Re_D and f vs. Re_D as shown in Figs. 9 and 10. The Type A and Type B inserts produce large increases in heat transfer coefficients over the smooth tube values. Coefficients are increased a lesser amount with the Type C insert.

Experiments were performed for horizontal and vertical orientations of the Type A and Type B inserts; the data are compared for each insert in Figs. 11 and 12. Performance differences for the two orientations are small except for the Type B turbulator at low Reynolds numbers where a slight decrease is found for the horizontal orientation.

Discussion

The Type A and turbulators produce about 150% increase in Nusselt number over a plain tube while the Type B turbulator provides about 12.% increase. The two turbulators are actually quite close in performance considering the measurement uncertainty. Also, operating conditions in actual boilers may make any difference of negligible importance. The Type C insert showed an increase in Nusselt number about 60 percent above that of the plain tube. Some visual observations, made with a plexiglass tube and smoke generator, indicated that the mixing was considerably better with the Type A and Type B turbulators than with the Type C insert.

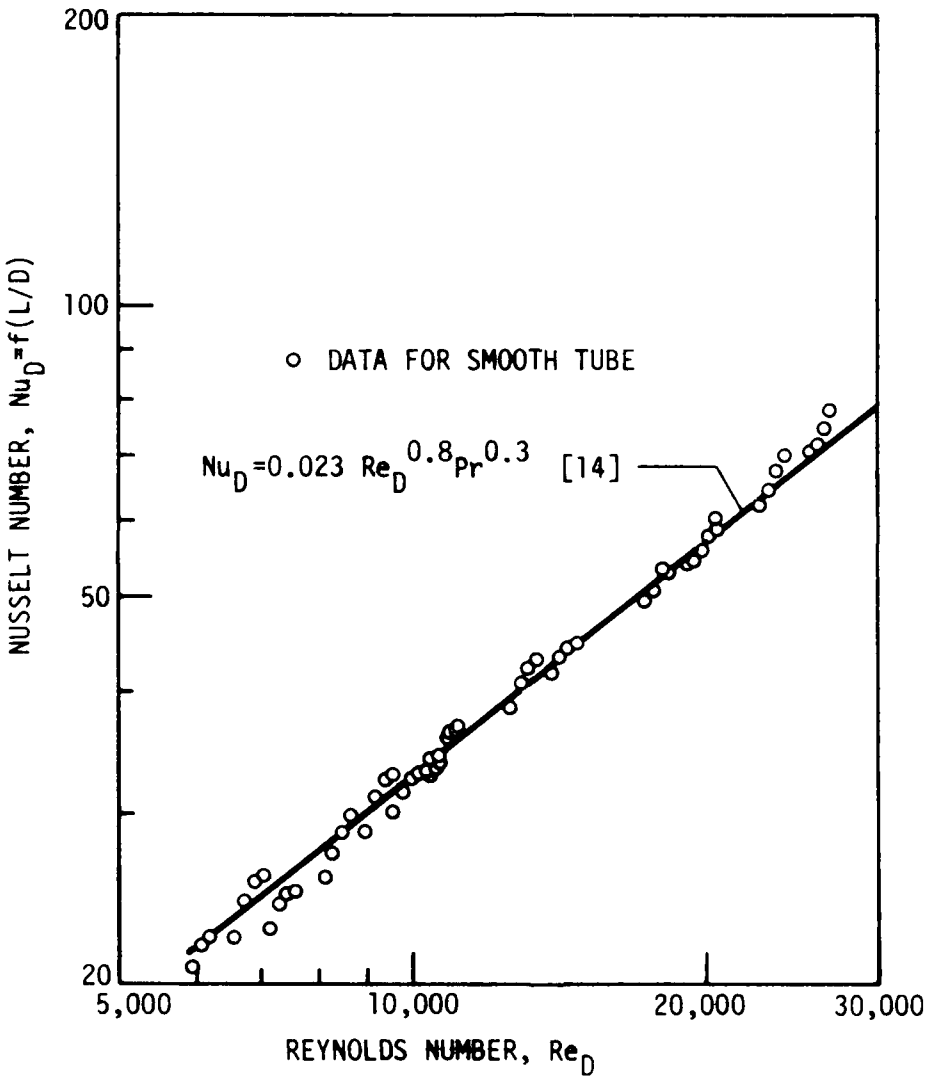

Fig. 8. Experimental data for smooth tube.

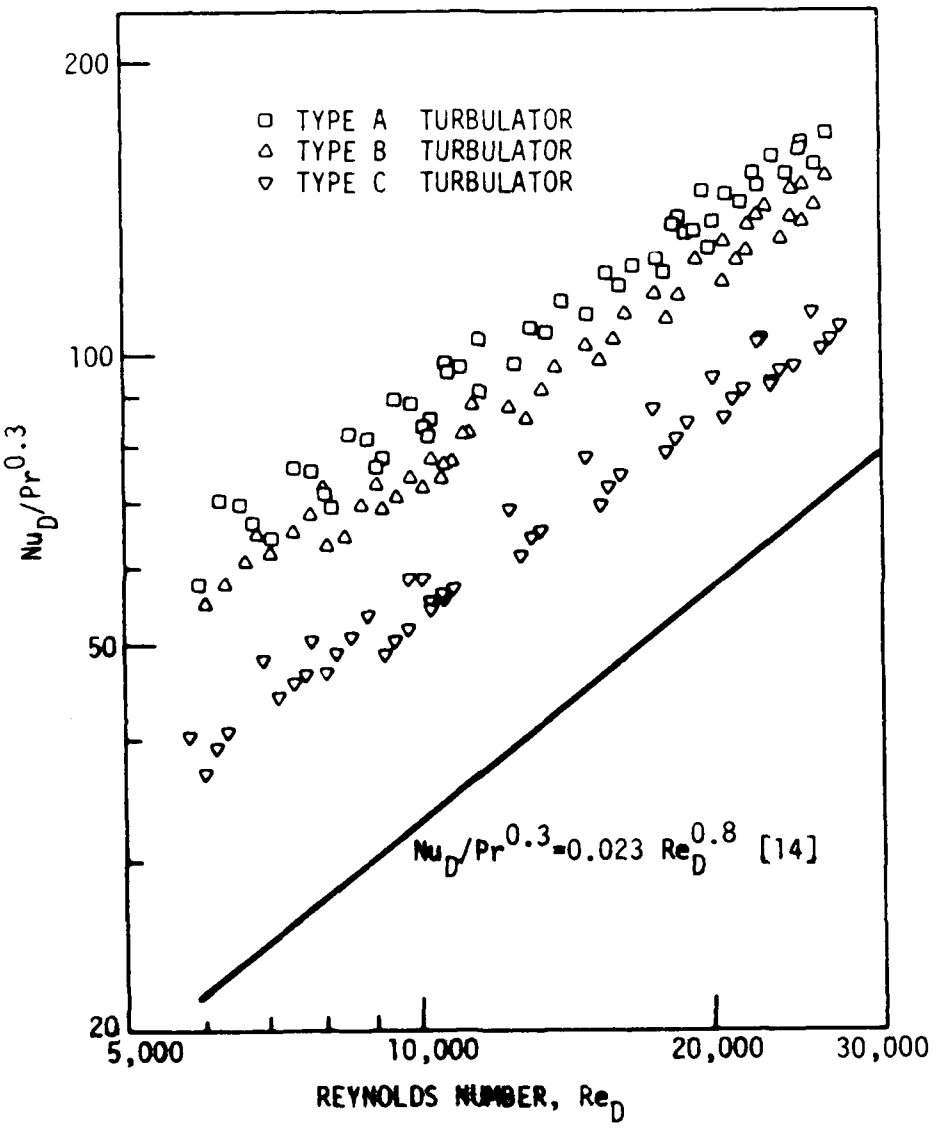

Fig. 9. Heat transfer data for Types A, B and C.

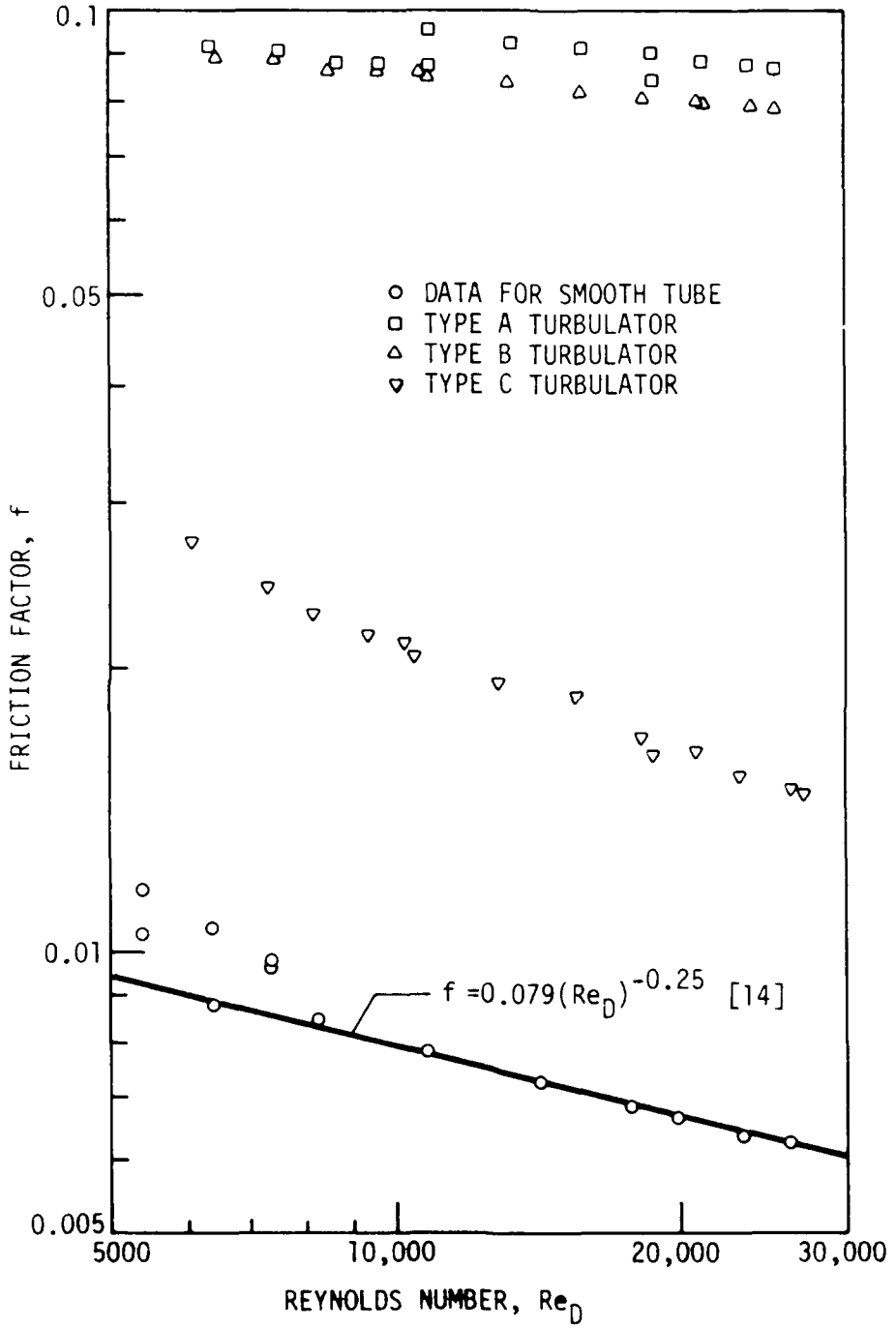

Fig. 10. Data for friction factor as defined in Eq. 5 for smooth tube and insert Types A, B and C.

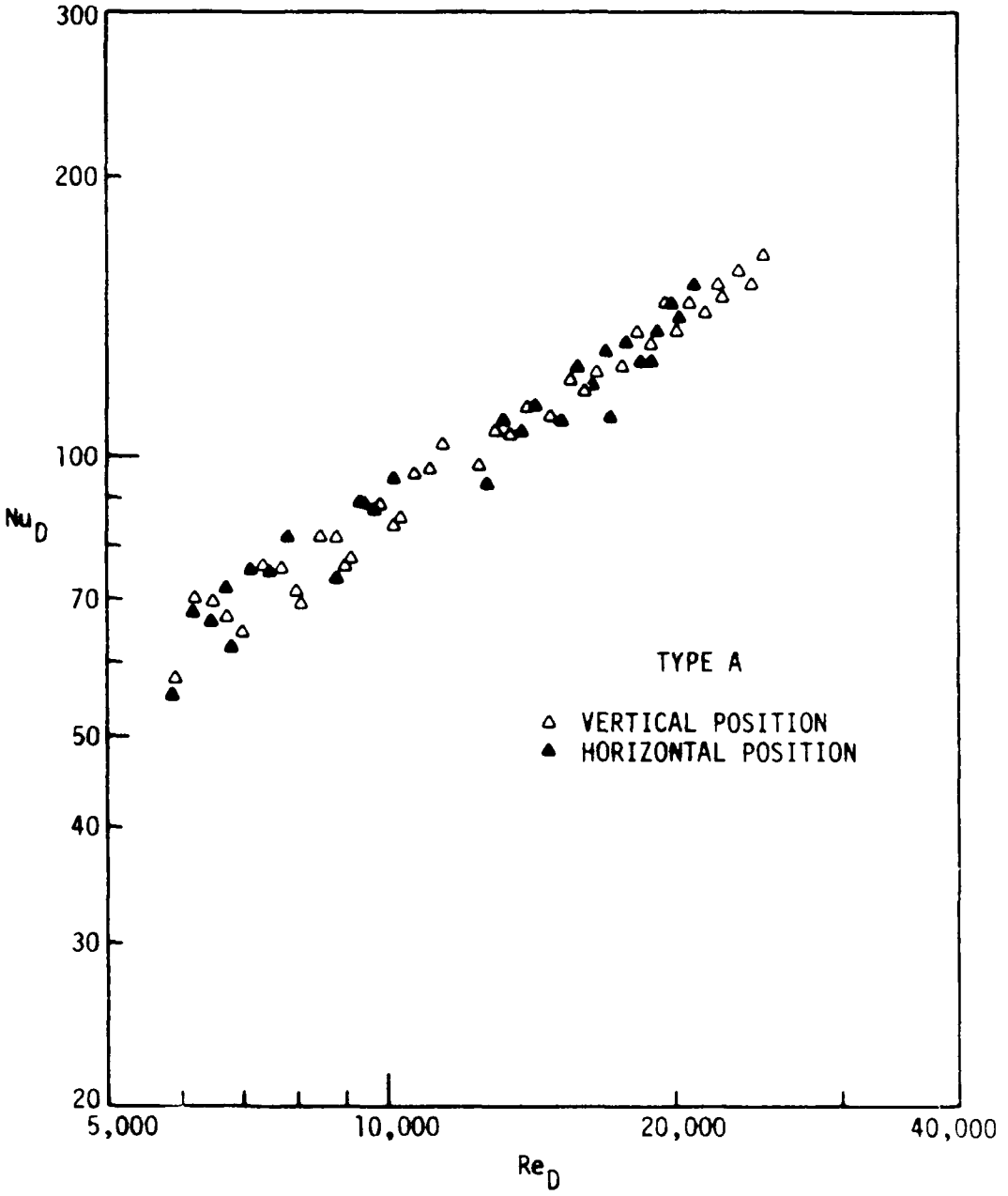

Fig. 11. Comparison of heat transfer data for vertical and horizontal orientation of insert Type A.

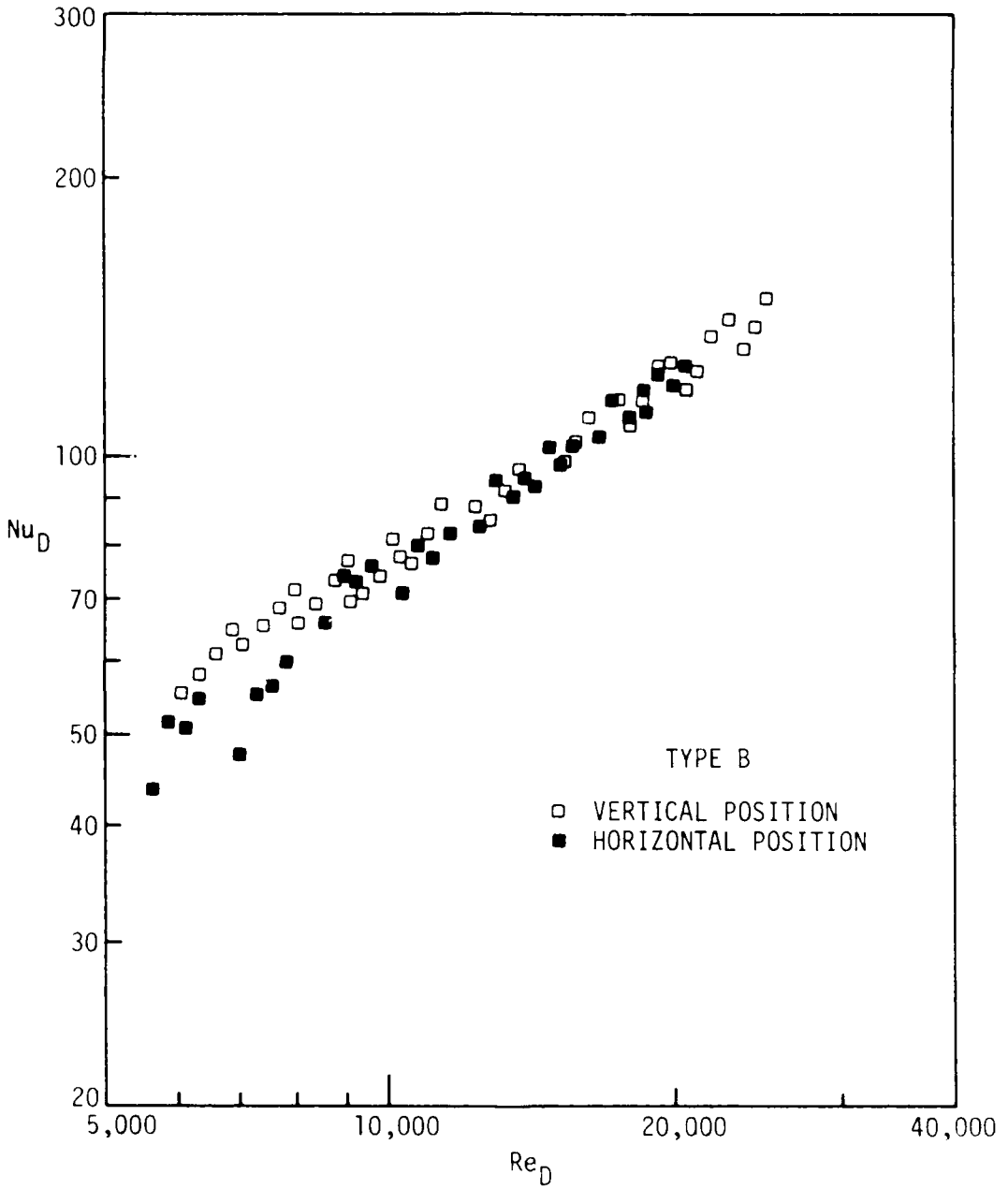

Fig. 12. Comparison of heat transfer data for vertical and horizontal orientation of insert Type B.

When the Type A and Type B inserts were positioned horizontally, the Nusselt number differences over the range of the Reynolds number tested are within experimental error except for the Type B insert between Reynolds numbers of 6,000 and 10,000. The difference was between 15 and 8% up to a Reynolds number of 10,000. At higher Reynolds numbers, the difference is negligible. It may be that in the horizontal orientation at lower Reynolds numbers, the mixing is not complete so that the hotter air travels along the upper part of the tube in a partially stratified flow. However, no detailed data were taken to confirm this speculation.

A review of the experimental data given in Table II for Reynolds numbers of 10,700 and 25,000 indicates more specifically the increases in Nusselt number and friction coefficient over plain tube data.

The friction coefficient for the Type A insert is 12.1 times that of a plain tube at a Reynolds number of about 10,000; the increase is 13.8 times at a Reynolds number of 25,000. The Type B insert has f increases of 11.0 and 12.4 times for the same Reynolds numbers, while the Type C insert has increases of 2.7 and 2.4 times, respectively, for these Reynolds numbers. The friction and heat transfer characteristics of the Type C insert are both comparable to data noted in the Literature Review.

When evaluating the relative merits of pressure loss cost for a particular heat transfer coefficient increase, it should be borne in

Table II. Nusselt number and friction coefficient increases

Insert Type	Re_D	Plain Nu_D	Plain f	Nu_D	f	Nu_D Ratio	f Ratio
Type A	10,700	39	.00785	100.4	.095	2.57	12.1
	25,000	76.5	.00630	180	.087	2.35	13.8
Type B	10,700	39	.00785	87.5	.086	2.25	11.0
	25,000	76.5	.00630	160	.078	2.09	12.4
Type C	10,700	39	.00785	62.5	.021	1.60	2.7
	25,000	76.5	.00630	110.1	.0151	1.44	2.4

mind that heat transfer can be enhanced considerably by merely increasing the air velocity with a concomitant increase in pressure loss. This situation, noted many years ago by Colburn and King [5], is a possible alternative to augmentation by use of inserts. Said differently, if a given increase in pressure loss is acceptable, it is possible to obtain the same augmentation by increasing the velocity (and the Reynolds number) to obtain a higher convective coefficient. However, this option is generally not available in a fire tube boiler.

Finally, it should be noted that a "fine scale" variation of Nusselt number as a function of Reynolds number may be discerned for each subsection of the test section, even though all data fall within the confidence bounds given. Sufficiently detailed tests to investigate and comment on this second-order phenomenon have not been included in this study. It was determined, however, that the temperature-dependent

property correction [Eqs. (1) and (2)] did not significantly reduce the scatter.

CONCLUSIONS

The results show that commercial turbulator inserts provide considerable enhancement of gas-side convective coefficients in fully-developed tube flow. It may be possible to reduce fuel consumption through the use of inserts, but improvement in gas-side convection coefficients does not result in a one-to-one ratio improvement in boiler efficiency. Rather, augmentation of gas side coefficients is only one factor among many items such as fuel/air ratio adjustment, tube cleanliness, and air/gas system flow resistance that help reach goals of reduced fuel consumption and improved boiler efficiency. It should further be noted that calculation of boiler efficiency with inserts should consider changes in the water side flow distribution (and heat transfer coefficient) brought about by the large increase in gas-side heat transfer coefficient.

ACKNOWLEDGMENTS

This study was sponsored by FESA under contract DAAK70-81-C-0219. The authors are indebted to Mr. James F. Thompson, Jr. of FESA and Dr. David A. Didion of the Center for Building Technology, National Bureau of Standards, for their assistance throughout the investigation.

REFERENCES

1. Bergles, A. E., Webb, R. L., Junkhan, G. H., and Jensen, M. K., "Bibliography on Augmentation of Convective Heat and Mass Transfer," Heat Transfer Laboratory Report HTL-19, ISU-ERI-Ames-79206, COO-4649-6, Iowa State University, Ames, Iowa, May 1979.

2. Whitham, J. M., "The Effect of Retarders in Fire Tubes of Steam Boilers," Street Railway Journal, Vol. 12, 1896, p. 374.

3. Kirov, N. Y., "Turbulence Promoters in Boiler Smoke Tubes," Journal of the Institute of Fuel, Vol. 22, 1949, pp. 192-196.

4. McDonald, R. J., Batey, J. E., Allen, T. W., and Hoppe, R. J., "Direct Efficiency Measurement and Analysis of Residential Oil-Fired Boiler Systems," Brookhaven National Laboratory, BNL 51171, November 1979.

5. Colburn, A. P. and King, W. J., "Relationship Between Heat Transfer and Pressure Drop," Industrial and Engineering Chemistry, Vol. 23, 1931, pp. 919-923.

6. Royds, R., Heat Transmission by Radiation, Conduction, and Convection, First Edition, Constable and Company, London, 1921, pp. 191-201.

7. Evans, S. I. and Sarjant, R. J., "Heat Transfer and Turbulence in Gases Flowing Inside Tubes," Journal of the Institute of Fuel, Vol. 24, 1951, pp. 216-227.

8. Thorsen, R. and Landis, F., "Friction and Heat Transfer Characteristics in Turbulent Swirl Flow Subjected to Large Transverse Temperature Gradients," Journal of Heat Transfer, Vol. 90, 1968, pp. 87-97.

9. Gee, D. L. and Webb, R. L., "Forced Convection Heat Transfer in Helically Rib-Roughened Tubes," Int. J. Heat Mass Transfer, Vol. 23, 1980, pp. 1127-1136.

10. Wassel, A. T. and Mills, A. F., "Calculation of Variable Property Turbulent Friction and Heat Transfer in Rough Pipes," Journal of Heat Transfer, Vol. 101, 1979, pp. 469-474.

11. Junkhan, G. H. and Bergles, A. E., "Heat Transfer Laboratory Data Acquisition System," Heat Transfer Laboratory Report HTL-12, ISU-ERI-Ames-77178, Iowa State University, Ames, Iowa, December 1976.

12. Dittus, F. W. and Boelter, L. M. K., "Heat Transfer in Automobile Radiators of the Tubular Type," Univ. of California (Berkeley) Publications in Engineering, Vol. 2, 1930, pp. 443-461.

13. Kline, S. J. and McClintock, F. A., "Describing Uncertainties in Single-Sample Experiments," Mechanical Engineering, Vol. 75, pp. 3-8.

14. Chapman, A. J., Heat Transfer, 3rd Edition, New York: Macmillan Publishing Co., 1974.

Appendix A: Insert Manufacturers or Distributors

A. Brock "Fuel Saver" Turbulator
Fuel Efficiency, Inc.
131 Stuart Avenue
P.O. Box 48
Newark, New York 14513
(Manufacturer)

B. Smick Turbulator
American Fuel Economy, Inc.
Rt. 1 Canal Rd. E.
Ottawa, Illinois 61350
(Manufacturer. Direct sales to boiler manufacturers)

AEI Fire Tube Turbulator
Allied Energy International
8601 Wilshire Blvd., Suite 1002
Beverly Hills, California 90211
(Retrofit distributor)

C. Powermaster Turbulator
Powermaster Corp.
P.O. Box 231
Middletown, Pennsylvania 17057
(Manufacturer)

Appendix B: Data Acquisition Flow Chart and Program

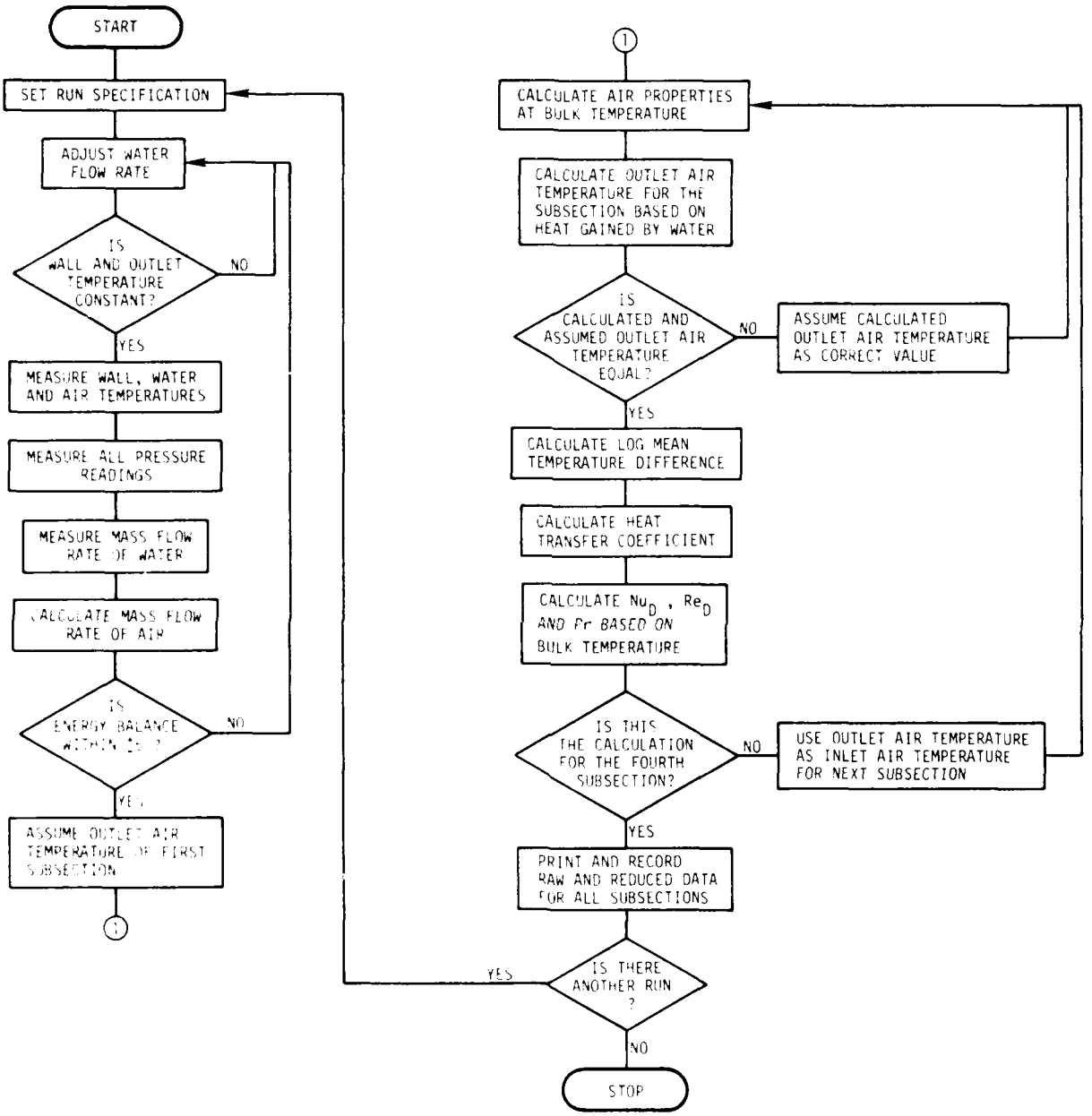

Fig. B-1. Data acquisition flow chart.

```
0: dim A$[15],B$[15],X$[15],X[17],D[47],A[11],B[11],F[11],G[11]
1: dim C[47],R[7],E[7]
2: wtb 6,32,32,32,32,32,32,32,32,32
3: wtb 6,27,77
4: dsp "Set printer at top of page";stp
5: wtb 6,27,84
6: wtb 6,27,70,int(1056/64),int(1056)
7: wtb 6,27,76,int(960/64),int(960)
8: ent "Operator?",A$
9: ent "Date?",B$
10: ent "Type of Run?",X$
11: fmt 1,"C",fz2.0,"E",z
12: fmt 2,"F1R3H0A1T1M3"
13: 0→C;wrt 709.1,C;wrt 722.2
14: for I=1 to 3
15: beep;dsp "Set scanivalve on channel",I;stp
16: if I=3;ent "Max. Pres. reached? Yes=1:No=0",N;if N=0;gto 18
17: if I=3;ent "Pres. in in.H2O?",D[32+I];gto 20
18: 0→K;for N=1 to 10;red 722,G;G+K→K;next N;K/10→C[32+I]
19: -1.139C[33]+1.139C[32+I]→D[32+I]
20: next I
21: beep;ent "Atmospheric pressure,in.Hg",C[39];C[39]→D[39]
22: fmt 3,"F1R2A1H1T1M3"
23: 32→C;wrt 709.1,C;wrt 722.3
24: 0→K;for N=1 to 10;red 722,G;G+K→K;next N;1000K/10→C[32]
25: 149.1195+44.1465C[32]+.0548C[32]^2-.0051C[32]^3→D[32]
26: (1.3259D[39]-.097527D[34])/(D[32]+459.67)→X[1]
27: 2.6866e-3(D[32]+459.67)^1.5/(D[32]+658.37)→X[2]
28: 15000→R[1];25000→R[2];35000→R[3];50000→R[4];75000→R[5];100000→R[6]
29: 150000→R[7];.02612→E[1];.02601→E[2];.02596→E[3];.02591→E[4];.02585→E[5]
30: .02582→E[6];.02579→E[7]
31: E[1]→B;R[1]→R
32: 12932.9505*B*√(X[1]*D[35])→M
33: 12.2525M/X[2]→S
34: if abs(S-R)<10;gto 40
35: for I=1 to 6
36: if S>R[I];gto 38
37: next I
38: E[I]-(S-R[I])*(E[I]-E[I+1])/(R[I+1]-R[I])→B
39: S→R;gto 32
40: M→X[3]
41: dsp "Mass flow,lbm/hr= ",X[3];stp
42: ent "Is Mass flow rate OK? Yes=1;No=0",N
43: if N=0;gto 11
44: dsp "Set Air Temperature";stp
45: fmt 3,"F1F2A1H1T1M3";fmt 1,"C",fz2.0,"E",z;wrt 722.3
46: 24→C;wrt 709.1,C
47: red 722,G;1000G→G;149.1195+44.1465G+.0548G^2-.0051G^3→G
48: dsp "Outlet Water Temp= ",G;wait 1000
49: dsp "Inlet Air Temp= ",F;wait 1000
50: 1→C;wrt 709.1,C
51: red 722,F;1000F→F;149.1195+44.1465F+.0548F^2-.0051F^3→F
52: dsp "To Record Data;STOP,cont57,EXC";wait 1000;gto 46
53: fmt 3,"F1R2A1H1T1M3";fmt 1,"C",fz2.0,"E",z;wrt 722.3
54: for I=1 to 32;1→C;wrt 709.1,C
55: 0→K;for N=1 to 10;red 722,G;G+K→K;next N;1000K/10→C[I]
56: 149.19950354+44.1464713C[I]+.05477916C[I]^2-.00509771C[I]^3→D[I]
57: next I
58: for I=1 to 4;I+32→C;wrt 709.1,C
59: 0→K;for N=1 to 10;red 722,G;G+K→K;next N;1000K/10→C[I+43]
```

Fig. B - 2. Data acquisition program.

```
60: 149.1995+44.1465C[I+43]+.0548C[I+43]^2-.0051C[I+43]^3+D[I+43]
61: next I
62: fmt 2,"F1R3H0A1T1M3"
63: 0→C;wrt 709.1,C;wrt 722.2
64: for I=1 to 6
65: beep;dsp "Set Scannivalve at Channel ",I;stp
66: if I=3;ent "Max. Pres. reached? Yes=1:No=0",N;if N=0;gto 68
67: if I=3;ent "Pres. in in.H2O?",D[32+I];gto 70
68: 0→K;for N=1 to 10;red 722,G;G+K→K;next N;K/10→C[I+32]
69: -1.139C[33]+1.139C[I+32]→D[I+32]
70: next I
71: ent "Enter Atmos.Pres. in.Hg",C[39];C[39]→D[39]
72: ent "Water flow ratein lbm/hr?",D[42]
73: D[42]→D[40]→D[41]→D[43]
74: (D[24]+D[25]+D[26]+D[27])/4→X[4]
75: (D[28]+D[29]+D[30]+D[31])/4→X[5]
76: X[4]-X[5]→X[6]
77: (X[4]+X[5])/2→r0
78: .2231+3.42e-5(r0+459.67)-2.93e-9(r0+459.67)^2→X[7]
79: (1.3259D[39]-.097527D[34])/(D[32]+459.67)→X[1]
80: 2.6866e-3(D[32]+459.67)^1.5/(D[32]+658.37)→X[2]
81: E[1]→B;R[1]→R
82: 12932.9505*B*(X[1]*D[35])→M
83: 12.2525M/X[2]→S
84: if abs(S-R)<10;gto 90
85: for I=1 to 6
86: if S>R[I];jmp 2
87: next I
88: E[I]-(S-R[I])*(E[I]-E[I+1])/(R[I+1]-R[I])→B
89: S→R;gto 82
90: M→X[3];B→X[13];S→X[15]
91: X[3]*X[7]*X[6]→X[8]
92: D[43](D[17]-D[16])→X[10]
93: D[42](D[19]-D[18])→X[12]
94: D[41](D[21]-D[20])→X[14]
95: D[40](D[23]-D[22])→X[16]
96: X[10]+X[12]+X[14]+X[16]→X[17]
97: .759255(D[47]-D[46])→X[9]
98: 1.071844(D[44]-D[45])→X[11]
99: X[4]→r9;X[3]→r10;X[16]-X[9]→r13;.971429→r16
100: (D[1]+D[2]+D[3])/3→A[3]→r14;(D[4]+D[5]+D[6])/3→A[4]→r15
101: cll 'nirm'(r9,r10,r11,r12,r13,r14,r15,r16,r17,r18,r19,r20,r21,r22)
102: r11→A[1];r12→A[2];r16→A[5];r17→A[6];r18→A[7];r19→A[8]
103: r20→A[9];r21→A[10];r22→A[11];A[1]→r9;X[14]→r13;1.030303→r16
104: A[4]→B[3]→r14;(D[7]+D[8]+D[9])/3→B[4]→r15
105: cll 'nirm'(r9,r10,r11,r12,r13,r14,r15,r16,r17,r18,r19,r20,r21,r22)
106: r11→B[1];r12→B[2];r16→B[5];r17→B[6];r18→B[7];r19→B[8]
107: r20→B[9];r21→B[10];r22→B[11];B[1]→r9;X[12]→r13;1.007407→r16
108: B[4]→F[3]→r14;(D[10]+D[11]+D[12])/3→F[4]→r15
109: cll 'nirm'(r9,r10,r11,r12,r13,r14,r15,r16,r17,r18,r19,r20,r21,r22)
110: r11→F[1];r12→F[2];r16→F[5];r17→F[6];r18→F[7];r19→F[8]
111: r20→F[9];r21→F[10];r22→F[11];F[1]→r9;X[10]-X[11]→r13;.992701→r16
112: F[4]→G[3]→r14;(D[13]+D[14]+D[15])/3→G[4]→r15
113: cll 'nirm'(r9,r10,r11,r12,r13,r14,r15,r16,r17,r18,r19,r20,r21,r22)
114: r11→G[1];r12→G[2];r16→G[5];r17→G[6];r18→G[7];r19→G[8]
115: r20→G[9];r21→G[10];r22→G[11]
116: dsp "Energy Balance = ",X[8]/X[17];stp
117: wrt 6,"Date: ",B$,"          ","Operator: ",A$
118: wrt 6,"Type of Run: ",X$
119: wrt 6,"-------------------------------- ----------------------"
```

Fig. B - 2. Continued.

```
120: wrt 6,"                              Raw Data"
121: wrt 6,"-------------------------------------------------------------"
122: wrt 6,"                          Temperature Data"
123: wrt 6,"Location                       Scanner     Reading          Temperature"
124: wrt 6,"                               Channel       Volts            deg.F"
125: wrt 6,"-------------------------------------------------------------"
126: fmt 5,2f12.6
127: wrt 6.5,"Test Sec.wall 1-top,C[1]    1    ",C[1],"        ",D[1]
128: wrt 6.5,"Test Sec.wall 1-ns,C[1]     2    ",C[2],"        ",D[2]
129: wrt 6.5,"Test Sec.wall 1-fs,C[3]     3    ",C[3],"        ",D[3]
130: wrt 6.5,"Test Sec.wall 2-top,C[4]    4    ",C[4],"        ",D[4]
131: wrt 6.5,"Test Sec.wall 2-ns,C[5]     5    ",C[5],"        ",D[5]
132: wrt 6.5,"Test Sec.wall 2-fs,C[6]     6    ",C[6],"        ",D[6]
133: wrt 6.5,"Test Sec.wall 3-top,C[7]    7    ",C[7],"        ",D[7]
134: wrt 6.5,"Test Sec.wall 3-ns,C[8]     8    ",C[8],"        ",D[8]
135: wrt 6.5,"Test Sec.wall 3-fs,C[9]     9    ",C[9],"        ",D[9]
136: wrt 6.5,"Test Sec.wall 4-top,C[10]  10    ",C[10],"        ",D[10]
137: wrt 6.5,"Test Sec.wall 4-ns,C[11]   11    ",C[11],"        ",D[11]
138: wrt 6.5,"Test Sec.wall 4-fs,C[12]   12    ",C[12],"        ",D[12]
139: wrt 6.5,"Test Sec.wall 5-top,C[13]  13    ",C[13],"        ",D[13]
140: wrt 6.5,"Test Sec.wall 5-ns,C[14]   14    ",C[14],"        ",D[14]
141: wrt 6.5,"Test Sec.wall 5-fs,C[15]   15    ",C[15],"        ",D[15]
142: wrt 6.5,"Water Inlet-4,C[16]        16    ",C[16],"        ",D[16]
143: wrt 6.5,"Water Outlet-4,C[17]       17    ",C[17],"        ",D[17]
144: wrt 6.5,"Water Inlet-3,C[18]        18    ",C[18],"        ",D[18]
145: wrt 6.5,"Water Outlet-3,C[19]       19    ",C[19],"        ",D[19]
146: wrt 6.5,"Water Inlet-2,C[20]        20    ",C[20],"        ",D[20]
147: wrt 6.5,"Water Outlet-2,C[21]       21    ",C[21],"        ",D[21]
148: wrt 6.5,"Water Inlet-1,C[22]        22    ",C[22],"        ",D[22]
149: wrt 6.5,"Water Outlet-1,C[23]       23    ",C[23],"        ",D[23]
150: wrt 6.5,"Air Inlet-1,C[24]          24    ",C[24],"        ",D[24]
151: wrt 6.5,"Air Inlet-2,C[25]          25    ",C[25],"        ",D[25]
152: wrt 6.5,"Air Inlet-3,C[26]          26    ",C[26],"        ",D[26]
153: wrt 6.5,"Air Inlet-4,C[27]          27    ",C[27],"        ",D[27]
154: wrt 6.5,"Air Outlet-1,C[28]         28    ",C[28],"        ",D[28]
155: wrt 6.5,"Air Outlet-2,C[29]         29    ",C[29],"        ",D[29]
156: wrt 6.5,"Air Outlet-3,C[30]         30    ",C[30],"        ",D[30]
157: wrt 6.5,"Air Outlet-4,C[31]         31    ",C[31],"        ",D[31]
158: wrt 6.5,"Room Temperature,C[32]     32    ",C[32],"        ",D[32]
159: wrt 6,"                          Pressure Data"
160: wrt 6,"                          -------------"
161: wrt 6,"Location                  Scannivalve   Reading          Pressure"
162: wrt 6,"                            Channel       Volts           in.H20"
163: wrt 6,"-------------------------------------------------------------"
164: wrt 6.5,"Atmosphere ref.,C[33]      1    ",C[33],"        ",D[33]
165: wrt 6.5,"St. inlet h.b.,C[34]       2    ",C[34],"        ",D[34]
166: wrt 6.5,"dp. orifice,C[35]          3    ",C[35],"        ",D[35]
167: wrt 6.5,"St. ds.orifice,C[36]       4    ",C[36],"        ",D[36]
168: wrt 6.5,"dp. test section,C[37]     5    ",C[37],"        ",D[37]
169: wrt 6.5,"st.ds. test sec.,C[38]     6    ",C[38],"        ",D[38]
170: wrt 6,"                       Keyboard Inputs"
171: wrt 6,"                       ---------------"
172: fmt 5,f12.6
173: wrt 6.5,"Atmospheric Pressure,C[39]              in.Hg      ",D[39]
174: wrt 6.5,"Water flow rate thru #1,C[40]          lbm/hr      ",D[40]
175: wrt 6.5,"Water flow rate thru #2,C[41]          lbm/hr      ",D[41]
176: wrt 6.5,"Water flow rate thru #3,C[42]          lbm/hr      ",D[42]
177: wrt 6.5,"Water flow rate thru #4,C[43]          lbm/hr      ",D[43]
178: wrt 6,"-------------------------------------------------------------"
179: wtb 6,12
```

Fig. B - 2. Continued.

```
180: wrt 6,"Date: ",B$,"          ","Operator: ",A$
181: wrt 6,"Type of Run: ",X$
182: wrt 6,"-------------------------------------------------------------"
183: wrt 6,"                    Reduced Run Data"
184: wrt 6,"-------------------------------------------------------------"
185: wrt 6.5,"Air density at orifice                lbm/cu.ft    ",A[1]
186: wrt 6.5,"Air viscosity at orifice              lbm/hr-ft    ",A[2]
187: wrt 6.5,"Air mass flow rate                       lbm/hr    ",X[3]
188: wrt 6.5,"Average inlet air temperature            deg.F     ",X[4]
189: wrt 6.5,"Average outlet air temperature           deg.F     ",X[5]
190: wrt 6.5,"Air temperaure drop                      deg.F     ",X[6]
191: wrt 6.5,"Specific heat of air           BTU/lbm-deg.F       ",X[7]
192: wrt 6.5,"Heat transfer from air                   BTU/hr    ",X[8]
193: wrt 6.5,"Heat transfer to water thru #4           BTU/hr    ",X[10]
194: wrt 6.5,"Heat transfer to water thru #3           BTU/hr    ",X[12]
195: wrt 6.5,"Heat transfer to water thru #2           BTU/hr    ",X[14]
196: wrt 6.5,"Heat transfer to water thru #1           BTU/hr    ",X[16]
197: wrt 6.5,"Total Heat transfer to water             BTU/hr    ",X[17]
198: fmt 5,f12.6
199: wrt 6.5,"Upstream temp.drop across teflon         deg.F     ",D[47]-D[46]
200: wrt 6.5,"Axial conduction from upstream           BTU/hr    ",X[9]
201: wrt 6.5,"downstream temp.drop across teflon       deg.F     ",D[44]-D[45]
202: wrt 6.5,"Axial conduction from downstream         BTU/hr    ",X[11]
203: sfg 14
204: wrt 6.5,"Energy Balance                                     ",X[17]/X[8]
205: wrt 6.5,"Outlet Air Temperature at #1             deg.F     ",A[1]
206: wrt 6.5,"Heat Tran. Coeff.-1        BTU/sq.ft-hr-deg.F      ",A[6]
207: wrt 6.5,"Nusselt Number-1                                   ",A[8]
208: wrt 6.5,"Prandtl Number-1                                   ",A[10]
209: wrt 6.5,"Reynolds Number-1                                  ",A[11]
210: wrt 6.5,"Outlet Air Temperature at #2             deg.F     ",B[1]
211: wrt 6.5,"Heat Tran. Coeff.-2        BTU/sq.ft-hr-deg.F      ",B[6]
212: wrt 6.5,"Nusselt Number-2                                   ",B[8]
213: wrt 6.5,"Prandtl Number-2                                   ",B[10]
214: wrt 6.5,"Reynolds Number-2                                  ",B[11]
215: wrt 6.5,"Outlet Air Temperature at #3             deg.F     ",F[1]
216: wrt 6.5,"Heat Tran. Coeff.-3        BTU/sq.ft-hr-deg.F      ",F[6]
217: wrt 6.5,"Nusselt Number-3                                   ",F[8]
218: wrt 6.5,"Prandtl Number-3                                   ",F[10]
219: wrt 6.5,"Reynolds Number-3                                  ",F[11]
220: wrt 6.5,"Outlet Air Temperature at #4             deg.F     ",G[1]
221: wrt 6.5,"Heat Tran. Coeff.-4        BTU/sq.ft-hr-deg.F      ",G[6]
222: wrt 6.5,"Nusselt Number-4                                   ",G[8]
223: wrt 6.5,"Prandtl Number-4                                   ",G[10]
224: wrt 6.5,"Reynolds Number-4                                  ",G[11]
225: wrt 6,"-------------------------------------------------------------"
226: beep;dsp "Insert tape and continue";stp
227: ent "Track 1 or 0?",T;trk T
228: ent "New tape? Yes=1:No=0",N
229: if N=1;gto 234
230: ent P
231: fdf P;idf Q,C,Q,C
232: if Q=0;gto 234
233: P+1→P;gto 231
234: fmt 6,f2.0,f3.0
235: wrt 6.6,"Tape Track=",T,"     Tape File=",P
236: dsp "Ready to mark and tape";stp
237: if N=1;jmp 2
238: fdf P
239: mrk 1,936
```

Fig. B - 2. Continued.

```
240: rcf P,A$,B$,X$,X[*],D[*],A[*],B[*],F[*],G[*]
241: dsp "Tape recorded";wtb 6,12;gto 10
242: end
243: "nirm":
244: p1+p3
245: .2231+3.42e-5((p1+p3)/2+459.67)-2.93e-9(p1+p3)^4+9.6^2+p4
246: if abs(p3-(p1-p5/p4/p2))<.1;gto 248
247: p1-p5/p4/p2+p3;gto 245
248: p8*p5*ln((p3-p7)/(p1-p6))/.990256(p3-p7-(p1-p6))+p8
249: 1/(1/p8-.004783)+p9
250: 1.3466e-2+2.2323e-5(p1+p3)/2+p10
251: 2.67p9/12/p10+p11
252: 2.6286e-3((p1+p3)/2+459.67)^1.5/((p1+p3)/2+658.5)+p12
253: p12*p4/p10+p13
254: 5.722425p2/p12+p14
255: ret
```

Fig. B - 2. Concluded.

Appendix C: Tabular Data

Table C - 1. Heat transfer data for smooth tube.

TYPE OF INSERT: No Insert

Re_D	Nu_D	Pr	Re_D	Nu_D	Pr
5806	24.02	0.705	11080	36.45	0.707
5947	21.97	0.706	11098	36.87	0.707
6074	22.11	0.707	12558	47.77	0.705
6200	22.26	0.707	12835	43.27	0.706
6574	27.69	0.705	13087	42.55	0.706
6735	25.82	0.706	13339	43.89	0.707
6884	25.69	0.706	13768	51.86	0.705
7031	25.87	0.707	14090	45.73	0.706
7115	28.16	0.705	14371	44.57	0.706
7283	25.38	0.706	14643	44.89	0.707
7433	24.79	0.706	17188	61.60	0.704
7580	24.84	0.707	17565	53.76	0.705
8105	31.91	0.705	17902	53.74	0.706
8280	28.95	0.706	18232	53.09	0.706
8441	28.97	0.707	19206	67.33	0.704
8605	29.96	0.707	19307	67.45	0.705
8929	35.65	0.705	19615	58.80	0.705
9126	32.87	0.706	19680	59.11	0.705
9311	32.62	0.706	19980	58.36	0.706
9500	32.85	0.707	20025	59.21	0.706
9534	37.22	0.705	20343	58.79	0.706
9751	33.43	0.706	20379	60.30	0.706
9947	32.85	0.706	22652	76.90	0.705
10140	32.70	0.707	23063	68.18	0.705
10382	42.25	0.704	23450	67.91	0.706
10420	40.86	0.705	23853	70.00	0.706
10641	34.96	0.705	25429	87.43	0.705
10652	35.74	0.705	25869	75.91	0.706
10865	36.12	0.706	26281	75.14	0.706
10871	36.36	0.706	26714	77.91	0.707

Table C - 2. Heat transfer data for Type A insert in vertical and horizontal orientations.

TYPE OF INSERT: Type A in vertical orientation

Re_D	Nu_D	Pr	Re_D	Nu_D	Pr
5916	57.90	0.706	13567	105.62	0.707
6228	70.48	0.707	14050	113.73	0.707
6515	69.82	0.707	14955	110.46	0.705
6752	67.00	0.707	15561	120.82	0.706
7049	64.76	0.706	16137	117.82	0.707
7408	76.21	0.707	16684	123.53	0.707
7735	75.69	0.707	17619	125.53	0.705
8008	71.63	0.707	17809	121.62	0.705
8105	69.37	0.705	18318	136.23	0.706
8488	82.55	0.707	18524	139.24	0.706
8849	81.87	0.707	18977	132.84	0.707
9039	76.22	0.705	19203	134.09	0.707
9159	77.86	0.707	19615	147.12	0.707
9450	89.62	0.707	19809	127.72	0.707
9840	88.49	0.707	20079	135.91	0.705
10180	83.96	0.707	20809	146.12	0.706
10244	81.82	0.705	21509	143.05	0.707
10287	85.59	0.705	22192	153.03	0.707
10720	97.28	0.706	22446	148.43	0.705
10724	95.88	0.707	23267	159.75	0.706
11143	96.27	0.707	23959	153.26	0.705
11170	95.45	0.707	24044	153.56	0.707
11543	103.58	0.707	24786	162.92	0.706
11558	90.32	0.707	24793	165.18	0.707
12533	97.36	0.705	25570	156.82	0.707
13064	107.08	0.706	26332	168.12	0.707

TYPE OF INSERT: Type A in horizontal orientation

Re_D	Nu_D	Pr	Re_D	Nu_D	Pr
5876	55.53	0.706	13866	106.74	0.707
6190	67.86	0.707	14349	113.89	0.707
6480	66.24	0.707	15258	109.87	0.705
6734	73.01	0.707	15876	125.66	0.706
6813	62.03	0.705	16464	118.61	0.707
7187	75.96	0.707	17018	130.09	0.707
7532	74.95	0.707	17157	111.36	0.705
7833	82.11	0.707	17808	132.81	0.706
8836	74.06	0.705	18446	127.04	0.707
9291	89.72	0.707	18871	127.53	0.705
9715	88.03	0.707	19051	136.95	0.707
10091	95.20	0.707	19592	147.66	0.706
12808	93.45	0.705	20290	141.51	0.707
13346	110.90	0.706	20954	154.02	0.707

Table C - 3. Heat transfer data for Type B insert in vertical and horizontal orientations.

TYPE OF INSERT: Type B in vertical orientation

Re_D	Nu_D	Pr	Re_D	Nu_D	Pr
6058	55.44	0.705	13368	91.47	0.707
6359	58.14	0.707	13805	96.41	0.707
6626	61.08	0.707	14901	102.01	0.705
6870	65.20	0.707	15447	98.30	0.706
7059	62.35	0.705	15957	103.27	0.707
7405	65.54	0.706	16473	110.45	0.707
7719	68.75	0.707	17510	115.80	0.705
8008	72.81	0.707	18128	108.84	0.706
8016	63.94	0.705	18702	115.17	0.707
8378	64.79	0.706	19290	125.76	0.707
8709	70.22	0.707	19982	127.34	0.705
9022	73.73	0.707	20542	130.38	0.706
9126	69.30	0.706	20648	118.26	0.706
9480	71.30	0.707	21192	125.67	0.706
9810	74.48	0.707	21266	124.81	0.707
10133	81.62	0.707	21793	127.78	0.707
10137	72.66	0.705	21899	135.48	0.707
10312	77.86	0.705	22391	138.33	0.707
10554	74.40	0.707	22878	141.52	0.705
10698	76.62	0.706	23596	131.84	0.706
10933	77.72	0.707	24263	147.61	0.705
11064	82.04	0.707	24266	138.89	0.707
11290	82.90	0.707	24952	149.57	0.707
11438	88.99	0.707	24992	136.37	0.706
12474	88.01	0.705	25671	142.58	0.707
12934	85.10	0.706	26366	152.38	0.707

TYPE OF INSERT: Type B in horizontal orientation

Re_D	Nu_D	Pr	Re_D	Nu_D	Pr
5635	43.83	0.705	12589	84.37	0.705
5898	51.43	0.706	13108	94.09	0.706
6147	50.96	0.707	13593	90.25	0.707
6374	54.65	0.707	14040	94.78	0.707
7025	47.73	0.705	14317	92.94	0.705
7325	56.77	0.706	14888	102.32	0.706
7616	56.50	0.707	15422	98.17	0.707
7887	60.05	0.707	15922	103.13	0.707
8582	66.37	0.705	16832	105.89	0.705
8986	74.28	0.706	17481	115.74	0.706
9359	73.26	0.707	18091	111.67	0.707
9697	76.53	0.707	18667	117.91	0.707
10391	71.06	0.705	18778	113.58	0.705
10840	80.04	0.706	19472	123.89	0.706
11256	77.85	0.707	20129	120.13	0.707
11637	82.72	0.707	20752	126.16	0.707

Table C - 4. Heat transfer data for Type C insert.

TYPE OF INSERT: Type C

Re_D	Nu_D	Pr	Re_D	Nu_D	Pr
5797	40.17	0.706	13028	64.58	0.706
6003	36.90	0.707	13390	65.37	0.707
6188	39.28	0.707	14846	77.87	0.704
6370	40.78	0.707	15304	69.57	0.706
6905	48.27	0.705	15718	72.65	0.706
7184	44.22	0.706	16132	74.54	0.707
7428	45.98	0.707	17457	87.36	0.704
7660	46.73	0.707	17957	78.80	0.706
7747	50.78	0.705	18417	81.40	0.706
8028	46.73	0.706	18882	84.16	0.707
8281	48.89	0.707	20026	94.44	0.705
8532	51.08	0.707	20549	85.64	0.706
8893	53.29	0.705	21039	89.32	0.706
9200	48.88	0.706	21541	91.06	0.707
9476	50.43	0.707	22427	102.18	0.705
9714	58.35	0.704	22626	102.41	0.705
9747	51.98	0.707	22987	92.56	0.706
10014	58.20	0.706	23182	93.24	0.706
10048	52.22	0.706	23507	94.05	0.706
10322	54.24	0.706	23701	95.58	0.706
10349	55.14	0.706	24034	96.46	0.707
10603	56.08	0.707	24228	97.01	0.707
10650	56.27	0.707	25441	110.87	0.705
10879	56.98	0.707	26023	101.19	0.706
12261	68.93	0.704	26573	103.69	0.706
12664	61.55	0.706	27140	107.75	0.707

Table C - 5. Friction data for heated runs.

TYPE OF INSERT: No Insert

Re_D	f
5381	0.0104
5408	0.0116
6382	0.0105
6385	0.0088
7352	0.0096
7353	0.0098
8227	0.0085
10754	0.0079
14218	0.0073
17722	0.0068
19786	0.0067
23254	0.0064
26073	0.0062

TYPE OF INSERT: Type A

Re_D	f
6353	0.0920
7550	0.0904
8650	0.0880
9627	0.0876
10923	0.0873
10924	0.0953
13303	0.0924
15834	0.0915
18632	0.0904
18836	0.0839
21147	0.0888
23638	0.0879
25162	0.0870

TYPE OF INSERT: Type B

Re_D	f
6478	0.0899
7548	0.0893
8531	0.0870
9637	0.0869
10729	0.0865
10878	0.0857
13145	0.0840
15694	0.0821
18407	0.0808
20949	0.0806
21479	0.0800
23923	0.0792
25323	0.0790

TYPE OF INSERT: Type C

Re_D	f
6090	0.0273
7294	0.0244
8147	0.0229
9329	0.0216
10190	0.0214
10454	0.0207
12836	0.0193
15500	0.0187
18178	0.0169
18805	0.0161
20789	0.0163
23239	0.0155
26294	0.0149
27098	0.0148

Appendix D: Sample Calculations and Uncertainty Analysis

Given below are equations used for calculation of experimentally-determined quantities necessary for determination of the surface convection coefficient $\bar{h}_a$ in one section of the calorimeter. Included is an uncertainty analysis of each calculated quantity obtained using the method of Kline and McClintock [13]; the measurement uncertainties used in this method are based primarily on instrumentation manufacturers specifications with odds of 20 to 1. Measurement uncertainties are given in Table D1. Use of necessary conversion factors to obtain compatible units is assumed.

Table D1. Uncertainties of measured quantities.

Variable	Uncertainty
Air temperature	±3°F
Water temperature	±0.4°F
Wall temperature	±0.4°F
Water flow rate	±0.75 lbm/hr
Properties of air ($C_{p,a}$, k_a, μ_a, P_r)	1%
Pressure	0.01 in. H_2O

Calculation of air density for orifice meter

$$\rho_a = \frac{p_{amb} + p_{st}}{R\ T_{st}}$$

The inputs for the run are:

p_{amb} = 29.04 in. Hg

p_{st} = 0.72 in. H_2O

T_{st} = 82.98°F

The result is ρ_a = 0.07086 lbm/ft^3

Calculation of uncertainty in air density

$$W_{\rho_a} = \left[\left(\frac{W_{p_{amb}}}{R\ T_{st}} \right)^2 + \left(\frac{W_{p_{st}}}{R\ T_{st}} \right)^2 + \left\{ -\frac{(p_{amb} + p_{st})}{R\ T_{st}^2}\ W_{T_{st}} \right\}^2 \right]^{1/2}$$

The result is W_{ρ_a} = 0.00013 lbm/ft^3

Calculation of air mass flow rate

$$\dot{m}_a = C_D \rho_a \sqrt{\frac{\Delta p_{or}}{\rho_a}}$$

The inputs are: C_D = 0.03692

Δp_{or} = 0.972 in. H_2O

ρ_a = 0.7086 lbm/ft^3

The result is $\dot{m}_a$ = 125.22 lbm/hr

Calculation of uncertainty in air mass flow rate

$$W_{\dot{m}_a} = \left[\left(\sqrt{\Delta p_{or}\ \rho_a}\ W_{C_D}\right)^2 + \left(\frac{C_D}{2}\sqrt{\frac{\Delta p_{or}}{\rho_a}}\ W_{\rho_a}\right)^2 + \left(\frac{C_D}{2}\sqrt{\frac{\rho_a}{\Delta p_{or}}}\ W_{\Delta p_{or}}\right)^2\right]^{1/2}$$

The result is $W_{\dot{m}_a} = 2.58$ lbm/hr

Calculation of energy gain by water

$$q_w = \dot{m}_w c_{p,w}(T_{w2} - T_{w1})$$

The inputs are: $\dot{m}_w = 65.76$ lbm/hr

$c_{p,w} = 1$ BTU/lbm-°F

$(T_{w2} - T_{w1}) = 22.67$°F

The result is $q_w = 1490.75$ BTU/hr

Calculation of uncertainty in energy gain by water

$$W_{q_w} = [(\dot{m}_w\ c_{p,w}\ W_{\Delta T_w})^2 + (c_{p,w}\ \Delta T_w\ W_{\dot{m}_w})^2 + (\dot{m}_w\ \Delta T_w\ W_{c_{p,w}})^2]^{1/2}$$

where ΔT_w refers to the temperature drop $(T_{w2} - T_{w1})$.

The result is $W_{q_w} = 57.25$ BTU/hr

Calculation of energy gain by conduction in calorimeter

$$q_c = k_t\ A\left(\frac{\Delta T_t}{\Delta X}\right)$$

The inputs are $k_t = 1.77$ BTU/hr-ft-°F

$A = 0.05$ ft^2

$\Delta T_t = 92.78$°F

$\Delta x = 1.4$ in.

The result is $q_c = 70.44$ BTU/hr

Calculation of uncertainty in energy gain by conduction

$$W_{q_c} = \left[\left(\frac{k_t A}{\Delta X} W_{\Delta T_t}\right)^2 + \left(\frac{A\Delta T_t}{\Delta X} W_{k_t}\right)^2 + \left(\frac{k\Delta T_t}{\Delta X} W_A^2\right) + \left(- \frac{kA\Delta T_t}{\Delta X} W_{A_x}\right)^2\right]^{1/2}$$

Considering, W_k, W_A, $W_{\Delta x} << W_{\Delta t}$

The result is W_{q_c} = 0.75 BTU/hr

Calculation of corrected energy gain by water

$$q_{w,c} = q_w - q_c$$

The inputs are: q_w = 1490.75 BTU/hr

q_c = 70.44 BTU/hr

The result is $q_{w,c}$ = 1420.31 BTU/hr

Calculation of uncertainty in corrected energy gain

$$W_{q,c} = W_{q_w} + W_c$$

= 58.0 BTU/hr

Calculation of outlet air temperature

$$T_{a2} = T_{a1} - \frac{q_{w,c}}{c_{p,a}\,\dot{m}_a}$$

The inputs are: T_{a1} = 318.52°F

$q_{w,c}$ = 1420.31 BTU/hr

$C_{p,a}$ = 0.2473 BTU/lbm-°F

$\dot{m}_a$ = 125.22 lbm/hr

The result is T_{a2} = 272.66°F

Calculation of uncertainty in outlet air temperature

$$W_{T_{a2}} = \left[\left(W_{T_{a1}} \right)^2 + \left(\frac{W_{q_{w,c}}}{c_{p,a} \dot{m}_a} \right)^2 + \left(\frac{q_{w,c}}{c_{p,a} \dot{m}_a^2} W_{\dot{m}_a} \right)^2 + \left(- \frac{q_{w,c} W_{c_{p,a}}}{\dot{m}_a c_{p,a}^2} \right)^2 \right]^{1/2}$$

The result is $W_{T_{a2}} = 3.69°F$

Calculation of log-mean temperature difference

$$\Delta T_{LMTD} = \frac{\Delta T_1 - \Delta T_2}{\ell n \frac{\Delta T_1}{\Delta T_2}} = \frac{(T_{a1} - T_{w2}) - (T_{a2} - T_{w1})}{\ell n \left(\frac{T_{a1} - T_{w2}}{T_{a2} - T_{w1}} \right)}$$

The inputs are $\Delta T_1 = 175.91°F$

$\Delta T_2 = 155.25°F$

The result is $\Delta T_{LMTD} = 165.36°F$

Calculation of uncertainty in log-mean temperature difference

$$W_{\Delta T_{LMTD}} = \left\{ \left[\frac{\ell n \left(\frac{\Delta T_1}{\Delta T_2} \right) - \left(\frac{\Delta T_1 - \Delta T_2}{\Delta T_1} \right)}{\left(\ell n \frac{\Delta T_1}{\Delta T_2} \right)^2} W_{\Delta T_1} \right]^2 + \left[\frac{\left(\frac{\Delta T_1 - \Delta T_2}{\Delta T_2} \right) - \ell n \left(\frac{\Delta T_1}{\Delta T_2} \right)}{\left(\ell n \frac{\Delta T_1}{\Delta T_2} \right)^2} W_{\Delta T_2} \right]^2 \right\}^{1/2}$$

The result is, $W_{\Delta T_{LMTD}} = 3.73°F$

Calculation of overall coefficient

$$U = \frac{q_{w,c}}{A_c \Delta T_{LMTD}}$$

The inputs are: $q_{w,c} = 1420.31$

$A_c = 1.02\ ft^2$

$\Delta T_{LMTD} = 165.36°F$

The result is $U = 8.76\ BTU/hr\text{-}ft^2\text{-}°F$

Calculation of uncertainty in overall coefficient

$$W_U = \left[\left(\frac{W_{q_{w,c}}}{A_c\ \Delta T_{LMTD}}\right)^2 + \left(\frac{-q_{w,c}}{A_c^2\ \Delta T_{LMTD}}\ W_{A_c}\right) + \left(\frac{-q_{w,c}}{A_c\ (\Delta T_{LMTD})^2}\ W_{\Delta T_{LMTD}}\right)^2\right]^{1/2}$$

The result is $W_U = 0.40\ BTU/hr\text{-}ft^{2\text{-}°F}$

Calculation of average heat transfer coefficient of air

$$\bar{h}_a = \frac{1}{\frac{1}{U} - \frac{D\ \ell n\left(\frac{D_t}{D}\right)}{2k_s}}$$

The inputs are, $D = 2.67$ in.

$D_t = 2.80$ in.

$k_s = 25\ BTU/hr\text{-}ft\text{-}°F$

$U = 8.76$

The result is $\bar{h}_a = 8.78\ BTU/hr\text{-}ft^2\text{-}°F$

Calculation of uncertainty in average heat transfer coefficient

$$W_{\bar{h}_a} = \left\{\left[\left(\frac{1}{U} - \frac{D\ \ln\left(\frac{D_t}{D}\right)}{2k_s}\right)^{-2}\left(\frac{-1}{U^2}\right)W_U\right]^2 + \left[\left(\frac{1}{U} - \frac{D\ \ln\left(\frac{D_t}{D}\right)}{2k_s}\right)^{-2}(-)\ \ln\left(\frac{D_t}{D}\right) - \frac{D^2}{2k_s}\ W_D\right]^2\right.$$

$$+\left[\left(\frac{1}{U}-\frac{D\ \ln\left(\frac{D_t}{D}\right)}{2k_s}\right)^{-2}\ \ \frac{D}{2k_s\ D_t}\ W_{D_t}\right]^2+\left[\left(\frac{1}{U}-\frac{D\ \ln\left(\frac{D_t}{D}\right)}{2k_s}\right)^{-2}(-)\ \frac{D\ \ln\left(\frac{D_t}{D}\right)W_{ks}}{2k_s^{\ 2}}\right]^2\Bigg\}^{1/2}$$

The result is $W_{\bar{h}a} = 0.4015$ BTU/hr-ft^2-°F

Calculation of Nusselt Number

$$Nu_D\ \ \frac{\bar{h}_a D}{k_a}$$

The inputs are: $\bar{h}_a = 8.78$ BTU/hr-ft^2-°F

$D = 1.67$ in.

$k_a = 0.0201$

The result is $Nu_D = 97.36$

Calculation of Reynolds Number

$$Re_D = \frac{4}{\pi}\frac{\dot{m}_a}{\mu_a D}$$

The inputs are: $\dot{m}_a = 125.22$ lbm/hr

$\mu_a = 0.05717$ lbm/ft-hr

$D = 2.67$ in.

The result is $Re_D = 12{,}533$

Calculation of uncertainty in Reynolds number

$$W_{Re_D} = \frac{4}{\pi}\left[\left(\frac{W_{\dot{m}_a}}{\mu_a D}\right)^2 + \left(\frac{-\dot{m}_a}{\mu_a D^2}\right)W_D^{\ 2} + \left(\frac{-\dot{m}_a}{\mu^2 D}\ \ W_{\mu_a}\right)^2\right]^{1/2}$$

The result is $W_{Re_D} = 287$

Calculation of correction for pressure drop due to temperature difference

$$\Delta p_c = \frac{\dot{m}_a}{A_x}\left(\frac{1}{\rho_{a1}} - \frac{1}{\rho_{a2}}\right)$$

where subscripts 1 and 2 refer to inlet and exit locations

The inputs are: $\dot{m}_a = 125.22$ lbm/hr

$\rho_{a1} = 0.04536$ lbm/ft^3

$\rho_{a2} = 0.06145$ lbm/ft^3

$A_x = 0.0389$ ft^2

$\Delta p_c = 0.03$ in. of H_2O

Calculation of the uncertainty in correction

$$W_{\Delta p_c} = \frac{1}{A_x}\left\{\left[2\dot{m}_a W_{\dot{m}_a}\left(\frac{1}{\rho_{a1}} - \frac{1}{\rho_{a2}}\right)\right]^2 + \left[\frac{-\dot{m}_a^2}{\rho_{a1}^2}\left(W_{\rho_{a1}}\right)\right]^2 + \left[\frac{-m_a^2}{\rho_{a2}^2} \quad W_{\rho_{a2}}\right]^2\right\}^{1/2}$$

The result is $W_{\Delta p_c} = 0.005$ in. H_2O

Calculation of corrected pressure drop across test section

$$\Delta p_f = \Delta p + \Delta p_c$$

The inputs are: $\Delta p = 0.41$ in. H_2O

$\Delta p_c = 0.03$ in. H_2O

The result is $\Delta p_f = 0.44$ in. H_2O

Calculation of uncertainty in corrected pressure drop

$$W_{\Delta p_f} = W_{\Delta p} + W_{\Delta pc}$$

The result is $W_{\Delta p_f} = 0.015$ in. H_2O

Calculation of friction factor

$$f = \frac{\Delta p_f}{\frac{\rho_a V^2}{8}} \frac{D}{L} = \frac{\pi^2}{16} \frac{\Delta p_f}{\dot{m}_a^2} \frac{\rho_a D^5}{L}$$

The inputs are: $\Delta p_f = 0.44$ in. H_2O

$\dot{m}_a = 125.22$ lbm/hr

$\rho_a = 0.05654$ lbm/ft^3

$D = 2.67$ in.

$L = 71.$ in.

The result is $f = 0.09243$

Calculation of uncertainty in friction factor

$$W_f = \frac{\pi^2}{16} \left\{ \left(\frac{W_{\Delta p_f} \rho_a D^5}{\dot{m}_a^2 L} \right)^2 + \left(\frac{\Delta p_f D^5 W_\rho a}{\dot{m}_a^2 L} \right)^2 + \left(\frac{\Delta p_f \rho_a 5D^4 W_D}{\dot{m}_a^2 L} \right)^2 \right.$$

$$\left. + \left(\frac{-\Delta p_{f\ a} \overset{5}{D} W_L}{\dot{m}_a^2 L^2} \right)^2 + \left(\frac{-2\ p_f \rho_a D^5 W_{\dot{m}_a}}{\dot{m}_a^3 L} \right)^2 \right\}^{1/2}$$

The result is $W_f = 0.0052$

LIST OF SYMBOLS

A area for conduction through teflon spacer

A_c empty tube surface area for calorimeter section

A_x cross sectional flow area of calorimeter section

C_D coefficient of discharge

$c_{p,a}$ specific heat at constant pressure of air

$c_{p,w}$ specific heat at constant pressure of water

D inside diameter of calorimeter pipe

D_t diameter of location of thermocouples in calorimeter pipe wall

fn_1 function of D and H in Eq. (1) from [8]

fn_2 function of D and H in Eq. (2) from [8]

H axial length for one full twist in Eqs. (1) and (2)

$\bar{h}_a$ average heat transfer coefficient for air

k_a thermal conductivity of air

k_s thermal conductivity of calorimeter wall

k_t thermal conductivity of teflon

L overall length of calorimeter (distance between pressure taps)

L_c heat transfer length of a calorimeter section

$\dot{m}_a$ mass flow rate of air

$\dot{m}_w$ mass flow rate of water

p pressure

p_{amb} ambient air pressure

p_{st} static air pressure

Δp measured pressure drop over calorimeter length

Δp_c correction to measured pressure drop over calorimeter length

Δp_f corrected pressure drop

Δp_{or} pressure drop across orifice

q_a energy given up by air

q_c energy loss by conduction in calorimeter

q_w energy gain by water

$q_{w,c}$ corrected energy gain by water

R ideal gas constant

T_{a1} inlet air temperature to a calorimeter section

T_{a2} outlet air temperature from a calorimeter section

T_b average air bulk temperature

$\bar{T}_s$ average wall (surface) temperature in a calorimeter section

T_{st} static temperature at orifice meter

T_{w1} inlet water temperature to a calorimeter section

T_{s2} outlet water temperature from a calorimeter section

ΔT_t temperature difference across teflon spacer

U overall heat transfer coefficient

ΔX teflon spacer thickness

W uncertainty, subscripted for each quantity for which the uncertainty is known or is to be calculated

Dimensionless parameters

f friction factor, defined in Eq. (5)

Gr Grashof number

Nu_D Nusselt number based on inside pipe diameter

Pr Prandtl number

Re_D Reynolds number based on inside pipe diameter

Greek symbols

ρ_a density of air

$\bar{\rho}_a$ average density of air

μ_a viscosity of air

SECURITY CLASSIFICATION OF THIS PAGE (When Data Entered)

REPORT DOCUMENTATION PAGE

READ INSTRUCTIONS BEFORE COMPLETING FORM

1. REPORT NUMBER: HTL-29, ISU-ERI-Ames-83130	2. GOVT ACCESSION NO.: AD-A150530
3. RECIPIENT'S CATALOG NUMBER:	
4. TITLE (and Subtitle): Tests of Turbulators for Fire Tube Boilers	5. TYPE OF REPORT & PERIOD COVERED: Final Report 29 September 1981-31 December 1982
	6. PERFORMING ORG. REPORT NUMBER: HTL-29
7. AUTHOR(s): C. E. Junkhan, A. E. Bergles, V. Nirmalan, T. Kavigururajan	8. CONTRACT OR GRANT NUMBER(s): DAAK-70-81-C-0219
9. PERFORMING ORGANIZATION NAME AND ADDRESS: Heat Transfer Laboratory, Dept. of Mechanical Engineering, Iowa State University, Ames, Iowa 50011	10. PROGRAM ELEMENT, PROJECT, TASK AREA & WORK UNIT NUMBERS
11. CONTROLLING OFFICE NAME AND ADDRESS: U.S. Army Facilities Engineering Support Agency, Engineering Division, Fort Belvoir, Virginia 22060	12. REPORT DATE: 10 December 1982
	13. NUMBER OF PAGES
14. MONITORING AGENCY NAME & ADDRESS (if different from Controlling Office)	15. SECURITY CLASS. (of this report): unclassified
	15a. DECLASSIFICATION/DOWNGRADING SCHEDULE

16. DISTRIBUTION STATEMENT (of this Report)

Approved for Public Release; Distribution Unlimited

17. DISTRIBUTION STATEMENT (of the abstract entered in Block 20, if different from Report)

18. SUPPLEMENTARY NOTES

19. KEY WORDS (Continue on reverse side if necessary and identify by block number)

Turbulators
Heat Transfer Augmentation
Heat Transfer Enhancement
Fire Tube Boilers

20. ABSTRACT (Continue on reverse side if necessary and identify by block number)

Heat transfer coefficients and friction factors were obtained for three turbulator inserts used in fire tube boilers. An electrically heated flow facility was developed to deliver hot air to a water-cooled steel tube of 2.675 in. i.d. and 71 3/4 in. length. Tube wall temperatures, fluid bulk temperatures, and flow rates were measured. The cooling coil was segmented so that sectional average heat transfer coefficients could be derived for four regions of the tube. (continued)

DD FORM 1 JAN 73 1473 EDITION OF 1 NOV 65 IS OBSOLETE

SECURITY CLASSIFICATION OF THIS PAGE (When Data Entered)

20.

Reference data for the empty tube are in excellent agreement with the usual correlations. Two commercial turbulators, consisting of narrow, thin metal strips bent and twisted in zig-zag fashion to allow periodic contact with the tube wall, displayed 125 and 157% increases in heat transfer coefficients at a Reynolds number of 10,700. Insert orientation had at most a 10% effect on the heat transfer coefficient. A third commercial turbulator, consisting of a twisted strip with width slightly less than tube diameter, provided a 60% increase in heat transfer coefficient. The friction factor increases accompanying these heat transfer coefficient increases were 1110%, 1000%, and 120%, respectively. These data should be helpful in assessing the overall performance gains to be expected when the turbulators are used in actual boilers.

AD-A150530

50272-101

REPORT DOCUMENTATION PAGE	1. REPORT NO. HTL-29 ISU-ERI-Ames-83130	2.	3. Recipient's Accession No.

4. Title and Subtitle
Tests of Turbulators for Fire-Tube Boilers

5. Report Date
October 1982

6.

7. Author(s)
G. H. Junkhan, A. E. Bergles, V. Nirmalan, and T. Ravigururajan

8. Performing Organization Rept. No.
HTL-29

9. Performing Organization Name and Address
Heat Transfer Laboratory
Department of Mechanical Engineering
Engineering Research Institute
Iowa State University
Ames, IA 50011

10. Project/Task/Work Unit No.

11. Contract(C) or Grant(G) No.
(C) DAAK 70-81-C-0219
(G)

12. Sponsoring Organization Name and Address
Department of the Army
U.S. Army Facilities Engineering Support Agency
Engineering Division
Fort Belvior, VA 22060

13. Type of Report & Period Covered
Final Report
9/29/81 - 12/31/82

14.

15. Supplementary Notes

16. Abstract (Limit: 200 words)

Heat transfer coefficients and friction facotrs were obtained for three turbulator inserts used in fire tube boilers. An electrically heated flow facility was developed to deliver hot air to a water-cooled steel tube of 2.675 in. i.d. and 71 3/4 in. length. Tube wall temperatures, fluid bulk temperatures, and flow rates were measured. The cooling coil was segmented so that sectional average heat transfor coefficients could be derived for four regions of the tube.

Reference data for the empty tube are in excellent agreement with the usual correlations. Two commercial turbulators, consisting of narrow, thin metal strips bent and twisted in zig-zag fashion to allow periodic contact with the tube wall, displayed 125 and 157% increases in heat transfer coefficients at a Reynolds number of 10,700. Insert orientation had at most a 10% effect on the heat transfer coefficient. A third commercial turbulator, consisting of a twisted strip with width slightly less than tube diameter, provided a 60% increase in heat transfer coefficient. The friction factor increases accompanying these heat transfer coefficient increases were 1110%, 1000%, and 120%, respectively. These data should be helpful in assessing the overall performance gains to be expected when the turbulators are used in actual boilers.

17. Document Analysis a. Descriptors

Turbulators
Heat Transfer Augmentation
Enhancement
Fire Tube Boilers,

b. Identifiers/Open-Ended Terms

c. COSATI Field/Group

18. Availability Statement:
No restriction on distribution
available from National Technical Information
Service, Springfield, VA 22151

19. Security Class (This Report)
UNCLASSIFIED

20. Security Class (This Page)
UNCLASSIFIED

21. No. of Pages
84

22. Price

(See ANSI-Z39.18)

See Instructions on Reverse

OPTIONAL FORM 272 (4-77)
(Formerly NTIS-35)
Department of Commerce

END

FILMED

3-85

DTIC